



ASSISTANCE IN BALANCE RECOVERY DURING GAIT USING AN ANKLE EXOSKELETON CONTROLLED WITH A NEUROMUSCULAR CONTROLLER.

G.F.Dedden, BSc.

FACULTY OF ENGINEERING TECHNOLOGY
DEPARTMENT OF BIOMECHANICAL ENGINEERING

EXAMINATION COMMITTEE

H.van der Kooij , prof.dr.ir.
E.H.F.van Asseldonk, dr.
G.A.Folkertsma, dr.ir.

DOCUMENT NUMBER
BW - 576

Preface

Before you lays the master thesis: "Assistance in balance recovery during gait using an ankle exoskeleton controlled with a neuromuscular controller". A balance study on the effects of a neuromuscular controller in both simulations and experiments. It is written to fulfil the master requirements of the master program: Biomedical Engineering at the University of Twente. I have performed research and wrote from November 2015 until August 2017.

The project was undertaken at the Department of Biomechanical Engineering at the University of Twente under the supervision of dr. E.H.F. van Asseldonk and Prof. dr. ir. H. van der Kooij. The research has led to a better insight of the subject and progress for empirical research. Due to several setbacks the research took longer than expected, because of parts which did not work out as supposed to be as the focus of the research has switched a few times.

I would like to thank my supervisors and all the persons from the Department of Biomechanical Engineering who have helped me during my experiments, especially ir. M.Vlutters and ir. A.Schreiber-Nijman. I would also like to thank my fellow students from the department for their support and inspiration. Lastly I would like to thank my family and friends who have always given me support when I needed it.

I hope you enjoy your reading

G.F.Dedden, BSc

Enschede, 24 August 2017

Abstract

Exoskeletons are a solution for assistance during gait and stance for people with spinal cord injury, as long as the right controller is used. Most controllers are not able to adapt to balance disturbances, due to being trajectory controlled. The neuromuscular controller is not trajectory controlled, but reflex based controlled and could possibly adapt to different disturbances. The effect of disturbances to the neuromuscular controller is not yet widely researched , hence this research.

The neuromuscular controller was tested on an ankle exoskeleton on balance control around the ankle when disturbed in forward and backward direction around the hip. Both simulations and experiments were used. The simulations consisted of forward simulations and data driven simulation, using pre-existing push response data as input, both simulations were compared to the pre-existing experimental data. For the experiment a healthy control subject was disturbed wearing an ankle exoskeleton using neuromuscular control. Responses were analysed on ankle torque and angle levels, EMG, controller variables and step variables.

The results show us that the controller does not assist in balance recovery. Instead if the controller will be used on impaired subjects the disturbance might be augmented, especially for the backward disturbance as there is additional torque in the opposite direction what is desired. Therefore further research for disturbances and the neuromuscular controller is recommended. Depending on these results parts or the whole controller should be changed to ensure safety for the wearer. A disturbance detection and a balance restoration module could be a solution as the controller is sufficient during normal gait but not during this specific disturbance.

Contents

1	Introduction	7
2	Methods and materials	8
3	Results	12
4	Discussion	16
5	Conclusion	18
6	Recommendations	18
	Appendices	i
A	Push simulations Geyer & Song's Model compared to experimental data	i
B	Data driven push simulation	vii
C	Calculation of inverse dynamics	ix
D	Additional figures	xi

List of Abbreviations

A	Activation or stimulation of muscle in neuromuscular controller	r_{foot}	Attachment radius of tendon on feet to the ankle
A_{SOL}	Activation of soleus muscle in neuromuscular controller	RHS	Right heel strike
A_{TA}	Activation of tibialis anterior muscle in neuromuscular controller	SCI	Spinal Cord Injury
ATP	Biological carrier of chemical energy	SE	Series element (tendon)
BE	Buffer elasticity, contractile element	SOL	Soleus
c	Describes magnitude at end of bell of the f_l curve	TA	Tibialis Anterior
CE	Contractile element (muscle)	T_{ankle}	Torque around the ankle
COM	Centre of mass	$t_{delayMid}$	Time delay middle
COP	Centre of pressure	$t_{delayLong}$	Time delay long
DOF	Degrees of freedom	v_{CE}	Velocity contractile element
EMG	Electromyography, the measurement of electrical activity of skeletal muscles	v_{max}	Maximum velocity contractile element
GAS	Gastrocnemius	ϵ	Muscle strain
G_{SOL}	Gain soleus in SOL feedback loop	ϵ_{ref}	Reference muscle stain
G_{SOLTA}	Gain soleus in TA feedback loop	ω	Reference strain
G_{TA}	Gain TA in TA feedback loop	ϕ_{ankle}	Angle between shank and feet
HAT	Head arms trunk segment	ϕ_{max}	Maximum angle between shank and feet
F_{be}	Force buffer elasticity	ϕ_{ref}	Angle between shank and feet where $l_{ce} = l_{opt}$
F_{ce}	Force contractile element		
F_{copx}	Horizontal force of the COP		
F_{copy}	Vertical force of the COP		
F_{grav}	Gravitational force of the foot		
f_l	Force length relation contractile element		
F_{mtc}	Mucle-tendon complex force		
F_{max}	Maximum muscle force		
F_{pe}	Force parallel elasticity		
F_{se}	Force series element		
f_v	Force velocity relation contractile element		
I	Moment of inertia of the feet		
K	Shape factor		
l_{CE}	Length contractile element		
l_{mtc}	Length muscle tendon complex		
l_{opt}	Optimum muscle length		
l_{SE}	Length series element		
l_{slack}	Minimum length of muscle without slack		
LTO	Left toe off		
MTC	Muscle tendon complex		
N	Eccentric force enhancement		
NMC	Neuromuscular controller		
PE	Parallel elasticity of contractile element		
$PreStim$	Minimal stimulation		
QOL	Quality of life		
$R(\sigma_{foot})$	Lever arm of muscle in correspondence to the joint		

General Introduction

In this report various concepts are used, which are not explained within the paper as they are considered background knowledge for experts in the area of Biomechanical assistance devices for SCI patients. Therefore these concepts will be introduced and explained (to a certain level) for those not familiar with the field. The following concepts will be elaborated on: Spinal cord injury (SCI), exoskeletons, muscle properties, movement terminology and the neural system.

As the name implies, spinal cord injury is an injury at the nerves in the spinal cord. An injury at the spinal cord can be temporarily or permanent. This can lead to loss of autonomic functions, loss of sense and loss of motoric functions. The amount of impairment depends on the level of the damage of the spinal cord and the severity of the lesion. If the lesion lies higher in the spinal cord more functions will be lost as the brain cannot communicate properly through nerves with the nerves connecting to the spinal cord below the lesion. If the lesion is partial, some functions will be lost while others are still maintained as there is still some neural communication possible. While with a full lesion all communication through nerves from the brain until below the lesion will be lost.

The most dangerous loss is the loss of autonomic function. Autonomic functions are functions in the human body which happen automatically without influence of one's consciousness. Autonomic function includes regulating heartbeat, digestion, urination and many other unconscious functions. If one of these functions is not working properly it could lead to inflammations and eventually cause the death of the person.

With sensory loss all feedback from the limbs is lost, this includes the loss of pain. Pain is often an indicator that something is wrong and should be solved. An example is a bladder infection. A bladder infection is something which often occurs in SCI patients as he/she cannot completely empty the bladder anymore due to not being able to voluntarily empty the bladder but is emptying the bladder passively (as there is no control through the nerves). In this case there is a high change on bladder inflammation. Bladder inflammation is often detected through pain during urinating. Though, if the pain is not detected due to the loss of sensory information, the bladder inflammation could have disastrous effects, ranging from a fever to organ loss and even death.

Lastly, motoric functions are usually lost. Motoric functions are conscious movements, for example walking or grasping movements. When the lesion is located higher in the spinal cord more motor functions are lost, while for lower locations less motor functions are lost. With a partial lesion some movement is still possible while with a full lesion movement like independent gait is not possible anymore.

A possible solution for loss of independent gait is an exoskeleton. An exoskeleton is a mechanical skeleton around the human body which can help to support movements, ranging from 0% to 100% support. These exoskeletons can also be used for various occasions, besides people with a SCI.

One of the other occasions is in the military. Here the exoskeletons are used to reduce the weight the soldiers otherwise have to carry themselves. This can mostly be used in areas where logistics via vehicles is not possible and supplies still have to be delivered. One of the armies using these exoskeletons is the US army.

Another application would be the training of impaired individuals to regain independent gait. An example would be the gait training of stroke patients. In conventional training 1-3 therapists are needed to give this type of training. The patient will walk on a treadmill while the therapists move the legs. This is very burdensome for the therapist and can therefore only be performed for a short therapy session. If a machine can assist with patient movement, the burden on a therapist will decrease and therefore the sessions can continue longer and can be more frequent.

Between the previous two occasions when using exoskeletons the requirements for the exoskeleton are completely different. For the military the exoskeletons need to be able to carry a lot of weight (which means that extra power is required) and should be usable in a lot of extreme environments (like a jungle (humid), desert (sand and extreme heat) and poles (extreme cold)), however, the control is a lot easier as it can be controlled with functional legs. Exoskeletons used for therapy need to work in a clean revalidation with a constant temperature and only need to hold the weight of the patient. Furthermore, as the patient does only need to walk, the exoskeleton can be fastened at a treadmill and be mounted at the ground making it possible to add larger motors and additional safety, through a safety harness attached above the patient. The control is however a lot more challenging as the legs are usually not (completely) functioning for control and therefore an algorithm should de-

side the movement. Though, normal human gait is highly variable and if this variability is not included, in the training will be less effective as the conventional training.

To gain independent gait for people without leg control, a combination of both the requirements of the occasions has to met. The exoskeleton should be able to move freely through space (so no fixed location as a treadmill nor a safety harness to a fixed location above the subject) and the controller should move the body without control through the legs of the person. If there is no control through the legs and there is no safety harness, balance and balance recovery becomes an issue in the control of the exoskeletons. As a SCI patient is not able to stand up after falling, it is of utmost importance that the balance and balance recovery are not an issue for the controller. This is easier said than done. With training exoskeletons the patient cannot fall due to a harness attached to the ceiling and walking on a treadmill (therefore the location is fixed). If it is an exoskeleton for daily use, and walking around the location is not fixed and the patient cannot be in a harness which is attached to the ceiling. Furthermore, when walking on a treadmill, no disturbances and other obstacles are present and the surface is straight. When walking on the road or in a home, obstacles will be present and the road will not be straight and other objects/people can bump into you causing a balance disturbance.

Most of the current controllers for exoskeletons follow a specific pattern, due to these set trajectories the controllers are not robust for balance (recovery). Therefore crutches are needed to stay balanced. A controller which does not use predefined trajectories is the neuromuscular controller. This controller attempts to mimic a muscle with a simple neural drive. In simulations, this controller already shows promising results, for normal gait and balance disturbances and is now being tested for prostheses and exoskeletons. This controller will be used for the experiments. In order to better understand this controller, the structure of a muscle will be explained and a general introduction to the nervous system will be given as a background. The specifics of the controller will be discussed in the method and materials of the report.

A skeletal muscle is made of muscle fibres, a muscle fibre consist among other things of myofibrils which consist of sarcomeres (figure 1). These sarcomeres consist of various proteins with the two most important ones myosin and actin (figure 1). When adding energy (ATP) to these two elements, it allows deattachment of the elements causing

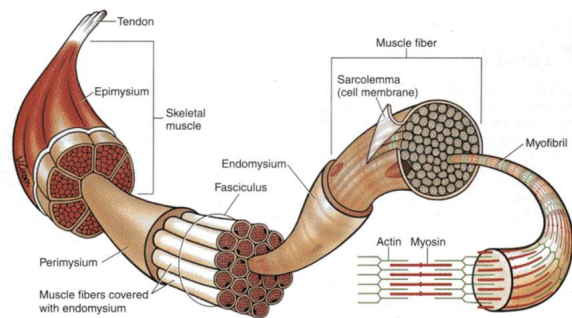


Figure 1: A schematic structure of the muscle, indicating the structure from the tendon and skeletal muscle to the active elements the actin and myosin [1].

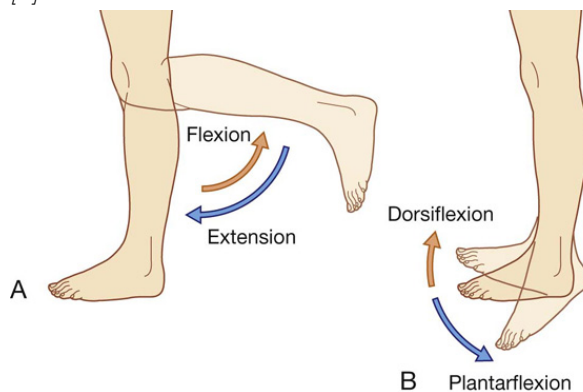


Figure 2: Human movements expressed in the anatomical terms of motion in the sagittal plane. The movements plantar flexion and dorsal flexion of the ankle and flexion and extension of the knee [2].

the elements to slide aside each other resulting in contraction or relaxation of the muscle. The actin and myosin are the actual active force conducting proteins of the muscle, the other elements in the sarcomere act as passive spring elements.

A muscle is attached to the bone (or another muscle) with a tendon. The relation between the active muscle part (actin and myosin), the passive muscle part (elements with spring behaviour) and the tendon (non-linear spring) are described with equations by the physiologist Archibald Vivian Hill and are known as Hills muscle model. In 1992, A.V.Hill received the Nobel Prize for his discovery and his model is still the golden standard for describing muscle behaviour. Therefore his equations are used for the muscle part of the neuromuscular controller.

As the muscle and tendon spans over at least one joint and is attached to at least 2 different bone structures it can move the different bones with respect to each other. As a muscle and tendon

can only pull, and an antagonistic muscle is used to perform the opposite movement. If a muscle is spanning over only one joint it causes usually only one type of movement. Examples are the tibialis anterior (TA) and the soleus (SOL). They are antagonist of each other and are spanning over the ankle joint. The tibialis causes dorsal flexion, which lifts the toes off the ground while the soleus causes plantar flexion, which pushes the toes to the ground (figure 2). A bi-articular muscle spans over two joints, an example is the gastrocnemius (GAS). This muscle causes plantar flexion in the ankle joint and flexion in the knee joint (figure 2).

All of the actions and movements of the human are send through the neural system. The total neural system can be split in the central nervous system and the peripheral nervous system. The central nervous system consist of the brain and the spinal cord, it is known as the central system as all decisions go through this system. The peripheral nervous system is the connection between the nervous system and organs or extremities.

Through neurological research we know a lot about how the neural system controls movement, but it is still not completely clear which part of the neural system directs which part of the gait. And especially what happens when there are disturbances during the gait. What causes the response of the body to the disturbance? It is not clear if this is a muscle reflex (reflex local in the muscle), spinal cord reflex (reflex trough the spinal cord) or a supra spinal cord reflex (reflex through brain). Which is why a part of the neuromusclar controller is made using assumptions and optimization methods.

1 Introduction

An exoskeleton could be used as a walking aid for many disorders. Spinal cord injury (SCI) is one of those disorders, with a prevalence of 252 per million citizens in Europe [3, 4]. With SCI there is a lesion at the spinal cord which disturbs nerve signals from the brain through the spinal cord to the corresponding muscles and backwards. This causes disappearing of feeling and control of the muscles, often resulting in loss of independent gait [5]. Loss of independent gait has a huge impact on the quality of life (QOL) and is one of the major problems resulting from a SCI. An exoskeleton could help to regain independent gait improving the QOL significantly.

Another way to regain independent gait would be to cure the lesion in the spinal cord. There are currently animal experiments where the lesion is sought to be cured and seem very promising [6]. Even though it seems promising, curing a lesion in animals and in humans are two different entities and it is not known if the same method also applies to humans. Even if it would work, similar lots of clinical experiments and clinical approvals will be needed what will take a lot of years. Alternatively, a walking aid could help a person regain gait. An exoskeleton is such an aid, this is a mechanical device which functions as an extra skeleton around the body. An exoskeleton can take over and/or support forces and torques normally provided by the legs. The biggest problem lies in the control of the exoskeleton. When and where is the force/torque supposed to act? Currently, there are exoskeletons that restore walking ability, though crutches are needed to keep balance. Therefore, the person cannot use the hands for e.g. carrying things, negatively influencing the QOL. A controller which could allow the user to use their hands is desired for an exoskeleton.

A reason the current control schemes do not work properly, is the type of control. Most schemes are based on trajectory control. This generally means that at a certain moment during gait either a certain torque or a certain angle must be achieved. This does not take into account external balance disturbances, different surfaces, variability between humans, variations in trunk/arm/head positions and/or extra ballast like a bag [7–10]. All these factors have an impact on the balance during gait. A promising approach, which does not use trajectory control, is mimicking neural control and muscle properties.

There are a few different theories for the neural gait control of humans. Two in particular: Spinal central pattern generators and neuromuscular control (NMC). The first theory assumes that the brain gives a signal to the spinal cord, that in turn creates a pattern of signals for gait, in order to decide the activation and force a muscle should generate at that moment in the gait cycle [11]. The second theorem is based on local muscle reflexes and muscle properties, better known as the hill muscle equations [12]. Here, the force velocity profile and the force length profile of a muscle plays an important role to simulate a muscle. The neural control is based on assumed reflexes between different muscles and the current phase of the gait cycle.

The last theorem is already successfully implemented in an active ankle prosthesis [13–15]. Moreover, simulations of NMC bipedal creatures seem quite robust under several disturbed circumstances [15, 16]. For different types of terrains and some external disturbances the NMC models can keep walking in a virtual environment [15, 16]. One of the biggest advantages is that the control does not depend on a predefined trajectory which leaves room for recovery after a disturbance.

Most of these promising results were acquired through simulations, however there are always some discontinuities between simulations and the real world [15]. An exact simulated representation of a human does not exist. Sensors in the simulation are usually perfect sensors and in the real world there are no perfect sensors, there is always some noise on the signal. However, by using simulations one can still give some predictions about reality and use it to optimize models. Accordingly, the NMC models might be robust in reality as well, but it has to be researched in an experimental setting.

The NMC used for the active ankle prosthesis is implemented on an ankle exoskeleton called Achilles [13–15, 17, 18]. This has been tested by a control subject during steady state walking. Here, they measured slightly lowered energetic cost and a slightly lowered muscle activity in the soleus (SOL) and tibialis anterior (TA). Furthermore, there were no large changes in walking dynamics of the subject except for a change in ankle angle [17]. These results imply that the NMC could be used for a lower limb exoskeleton during normal gait. However the response to balance disturbances is not researched in depth yet, hence this paper.

In this paper the response of the NMC around the ankle will be tested on two specific disturbances. The disturbance will be around the hip in forward and backward direction at right

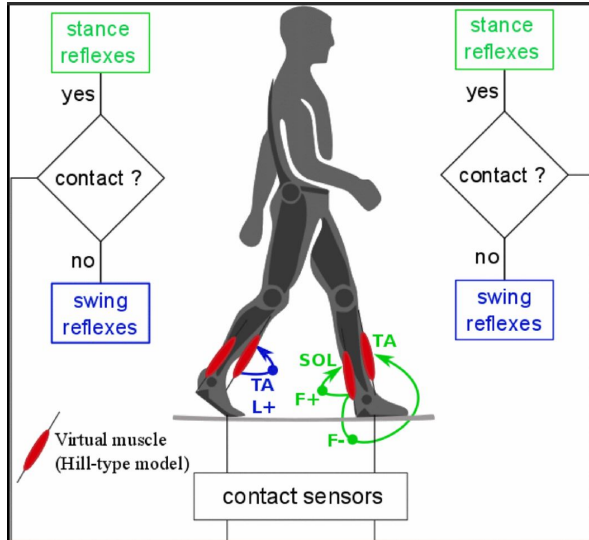


Figure 3: A schematic overview of the NMC when implemented within Achilles (the ankle exoskeleton) in the experiments [17].

feet toe off. From simulations a prediction of the response was made. Here, the NMC did not do the same as a human (Appendix A and B). The response is different in magnitude, where extra plantar flexion is desired less plantar flexion is generated and where dorsiflexion is desired extra plantar flexion is generated. It is however known that a human changes their gait when aided with NMC around the ankle [17, 19], therefore the response of a healthy human with NMC assistance around the ankle during perturbations is not known and therefore tested.

Two simulation were calculated before the main experiments. The first simulation was done by simulating a simple push in an already existing NMC simulation [15](Appendix A). From this forward simulation a small response to the disturbance could be seen, though the human has a larger response. Furthermore, when the human would perform dorsion flexion the model would create additional plantar flexion (in comparison to normal gait) and when the human does extra plantar flexion, the model does less plantar flexion (in comparison to normal gait). For the human data during normal gait the results from Vlutters et al. was used [20]. Their experimental setup was the same, except that no ankle exoskeleton was used. For the second simulation the data from Vlutters et al. was again used [20]. The ankle angles from those experiments were used as input for the NMC in an off-line data driven simulation(Appendix B). In this data-driven simulation the response was the same as the forward simulation except that the response

was much larger, with the biggest difference the over 100Nm plantar flexion, while dorsion flexion was desired (appendix B. The experimental set-up adds only the ankle exoskeleton with NMC to the experimental set-up of Vlutters et al. [20], with the controller used for the steady state walking experiments from Dzeladini et al., the same controller is also used for the data driven simulation [17].

From the simulations we expect that the neuromuscular controller would augment the disturbance [20] (Appendix A and B). Causing the balance recovery to be worse and also changing the angle and torque values. Also, it is unknown if a subject will learn to adapt to the aid of the controller when disturbed, therefore 8 pushes before a training period and after the training period are compared to check if there are any differences.

2 Methods and materials

Neuromuscular Controller (NMC)

The NMC is based on properties of the muscle tendon complex (MTC) and nerve system. The NMC uses joint angles, joint angular velocity and phase of the gait as external inputs (figure 4). Based on the MTC and nerve properties, the model will calculate a muscle force. The muscle force, muscle attachment and joint angle will then determine the torque applied on the joint by the muscle. The summation of all the torques on one joint will be the torque that the exoskeleton should provide on that joint [13–15]. The whole model is the same as used in Dzeladini et al. [17] which is implemented from the model designed by Geyer & Song [13, 14].

The controller will be explained with as basis the scheme in figure 4. This figure is a representation of the torque provided by a single muscle. The scheme will be explained in: Muscle Attachment Geometry, Muscle Tendon Complex and the Activation of the muscle. Note that for some muscles there will be slight deviations from the scheme provided in figure 4, as muscles are not always exactly the same. Furthermore, joint limits are applied to prevent overextension of the ankle.

The gastrocnemius (GAS) was not included in the controller as this muscle is bi-articular (spans over the knee and ankle joint) and needs input from the knee angle what is not

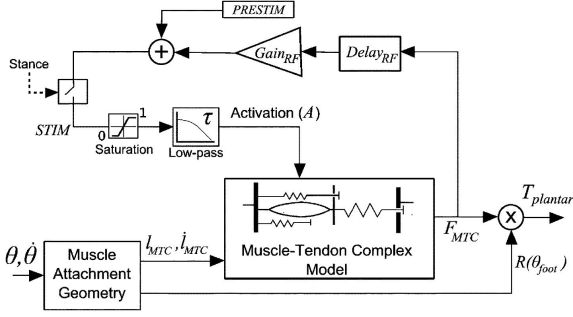


Figure 4: A scheme of the NMC for one muscle [14] including the muscle-tendon complex model, the muscle attachment geometry and the activation are elaborated in the text. Take note that for some muscles the activation part of the muscle can be different as some muscles have different feedbacks.

provided by this particular ankle exoskeleton. The Soleus (SOL) and Tibialis Anterior (TA) are monoarticular which only spans over the ankle, the ankle angle is provided by the ankle exoskeleton. As the Soleus and Tibialis Anterior are antagonist of each other, one of the two forces has to be subtracted from the other. The soleus causes plantar flexion at the ankle, while the tibialis anterior causes dorsal flexion at the ankle. After the torque for each muscle is calculated the torque provided around the ankle will be calculated as followed:

$$T_{ankle} = T_{sol} - T_{TA} \quad (1)$$

Muscle attachment geometry of one muscle

The lever arm ($R(\sigma_{feet})$) multiplied with the force of the MTC (F_{mtc}) is the torque provided by the muscle around the ankle joint. The lever arm and the input of the MTC (the length of the MTC l_{mtc}) is depending on the ankle angle and its attachment to the bone. Both variables are calculated in the muscle attachment geometry (figure 4). The lever ($R(\sigma_{feet})$) is calculated as followed:

$$R(\phi_{ankle}) = \cos(\phi_{ankle} - \phi_{max})r_{foot} \quad (2)$$

With ϕ_{ankle} as the angle between the shank and the feet, ϕ_{max} at which is the maximum ankle muscle-tendon arm and the attachment radius r_{foot} .

The length of the MTC l_{mtc} is calculated as followed:

$$l_{mtc} = \rho r_{foot} [\sin(\phi_{ref} - \phi_{max}) - \sin(\phi_{ankle} - \phi_{max})] \quad (3)$$

Where ρ represents the pennation angle of the muscle fibers with respect to the tendon and ϕ_{ref} is the angle where $l_{ce} = l_{opt}$.

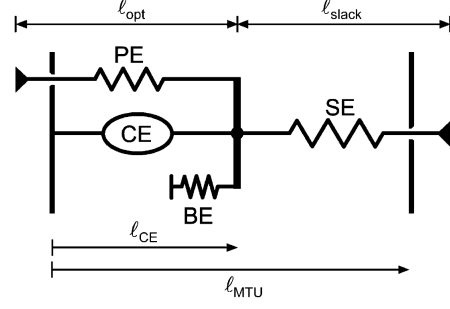


Figure 5: A scheme of the muscle-tendon complex (MTC). The CE is the active element of the muscle, the PE and BE are the passive elements of the muscle and the SE is a representation of the tendon. [13].

Muscle-tendon complex model

The MTC is the most complex part of the model. In here the tendon (SE) and the sarcomeres (contractile element = CE) and the passive muscle elements (PE and BE) are modelled. The formulas are based on the Hill muscle model equations. Using the scheme in figure 5 the virtual muscle force (F_{mtc}) can be calculated using the following elements [13, 14]:

$$F_{mtc} = F_{se}(l_{se}) = F_{ce}(l_{ce}, v_{ce}, A) + F_{pe}(l_{ce}) - F_{be}(l_{se}) \quad (4)$$

Where F_{mtc} is the individual muscle force, which is in series with the tendon (SE). Therefore the force of the tendon (F_{se}) is equal to the force of the contractile element (F_{ce}) and a combination of passive linear properties of the muscle which also limits the maximum muscle length, this expressed in (F_{pe} and F_{be}).

The tendon force (F_{se}) of the MTC is calculated as followed [13, 14]:

$$F_{se} = \begin{cases} F_{max}(\frac{\epsilon}{\epsilon_{ref}})^2 & \epsilon > 0 \\ 0 & \epsilon \leq 0 \end{cases} \quad (5)$$

Where ϵ the muscle strain is calculated as followed:

$$\epsilon = \frac{l_{se} - l_{slack}}{l_{slack}} \quad (6)$$

If the $\epsilon < 0$, there is no pull and as the tendon can only pull the $F_{se} = 0$. When there is a pull the tendon will act as a non-linear spring (equation 5), with as input the strain which is dependent on the length of the tendon (l_{se} , equation 7). Furthermore, the force of the tendon is dependent on the maximum force of the muscle F_{max} and the reference strain ϵ_{ref} the rest length of the tendon l_{slack} . The length of the SE (l_{se}) is calculated as followed [13]:

$$l_{se} = l_{mtc} - l_{ce} \quad (7)$$

With l_{mtc} as the length of the MTC (equation 3) and l_{ce} (equation 9) as the length of the contractile element.

The force generated by the contractile part of the muscle (F_{ce}) is calculated using [13, 14]:

$$F_{ce} = A \cdot F_{max} \cdot f_l(l_{ce}) \cdot f_v(v_{ce}) \quad (8)$$

Where $f_v(v_{ce})$ is the force-velocity relation of the muscle (equation 10), where v_{ce} is the velocity that the length of the CE is changing and is integrated to get the l_{ce} (equation 9), $f_l(l_{ce})$ is the force-length relation of the muscle (equation 11) and A is the activation (most similar to EMG, see equation 15 and 14).

As integrating is more stable in simulations the v_{ce} will to the l_{ce} in the model [14]:

$$l_{ce} = \int v_{ce} dt + l_{ce_{t=0}} = \int [f_v(v_{ce})]^{-1} dt + l_{ce_{t=0}} \quad (9)$$

Where the initial condition $l_{ce_{t=0}}$ is equal to $l_{slack} - l_{mtc_{t=0}}$ and the force-velocity (f_v) equation is as followed [13]:

$$f_v(v_{ce}) = \begin{cases} (v_{max} - v_{ce}) \setminus (v_{max} + KV_{ce}) & v_{ce} < 0 \\ N + (N - 1) \frac{v_{max} + v_{ce}}{7.56Kv_{ce} - v_{max}} & v_{ce} \geq 0 \end{cases} \quad (10)$$

Where K is the shape factor, N is the eccentric force enhancement and v_{max} is the maximum velocity of the CE (Note: F_v cannot be below or equal to 0).

The force-length relation f_l is described with the following formula [13]:

$$f_l(l_{ce}) = \exp \left[c \left| \frac{l_{ce} - l_{opt}}{l_{opt}w} \right|^3 \right] \quad (11)$$

The l_{opt} is the optimal length for the maximum force of the muscle and w is the reference strain.

The two passive muscle elements, the parallel elasticity (F_{pe}) and the buffer elasticity (F_{be}) are calculated as followed [14]:

$$F_{pe} \begin{cases} F_{max} \left[\frac{l_{ce} - l_{opt}}{l_{opt}w} \right]^2 f_v(v_{ce}) & x = 0 \\ 0 & otherwise \end{cases} \quad (12)$$

$$F_{be}(l_{ce}) = \begin{cases} F_{max} \left[\frac{l_{ce} - (1-w)}{l_{opt}w/2} \right]^2 & l_{ce} \leq l_{opt}(1-w) \\ 0 & otherwise \end{cases} \quad (13)$$

Table 1: Parameters used in the NMC, these parameters are taken from the model used by Dzeladini et al. and used for the controller in the experiment. Take note that some parameters are different between different muscles [17].

General Parameters		
MTC		
w [m]	0.56	
c []	0.05	
N []	1.5	
K []	5	
Activation		
LongDelay [s]	0.020	
ShortDelay [s]	0.010	
PreStim	0.01	
G_{SOL} [1/N]	$1.2/F_{max,sol}$	
G_{TA} [1/N]	1.1	
G_{SOLTA} [1/N]	$0.4/F_{max,sol}$	
PreStim []	0.01	
Joint stop		
Lower [rad]	$70\pi/180$	
Higher [rad]	$130\pi/180$	
Muscle specific parameters		
Attachments		
	SOL	TA
r_{foot} [m]	0.05	0.04
ϕ_{max} [rad]	$110\pi/180$	$80\pi/180$
ϕ_{ref} [rad]	$80\pi/180$	$100\pi/180$
MTC		
	SOL	TA
F_{max} [N]	4000	800
l_{opt} [m]	0.04	0.06
v_{max} [m/s]	6	12
l_{slack} [m]	0.27	0.23

Activation (A) or the neural activation for specific muscles

The activation (A) is a representation of the neural activation. The A is dependent on the phase of the gait and sometimes on different muscles. The activation is limited from 0.01 to 1 as there is also a limit to activation of a muscle in reality. Between the activation and the muscle input is a delay ($t_{delayLong}$) present as the neural network in reality also has a delay, just as for the gait phase also has a delay ($t_{delayMid}$). The activation of the TA (A_{TA}) and SOL (A_{SOL}) are calculated as followed [14]:

$$A_{TA} = \begin{cases} PreStim - \\ F_{MTC,SOL}G_{SOLTA} + L_{ce,TA}G_{TA} & Stance \\ PreStim + L_{ce,TA}G_{TA} & Swing \end{cases} \quad (14)$$

Table 2: General subjects characteristics of the subjects whose data is used in the results.

Age [years]	Mean: 25	Std:1
Leg length [m]	Mean:0.99	Std:0.05
Length [m]	Mean:1.76	Std:0.09
Weight [kg]	Mean:66	Std:10
Experience Achilles	yes: 1 , no: 5	
Experience pusher	yes: 3 , no: 3	
# of subjects	female: 5 , male: 1	

$$A_{SOL} = \begin{cases} Pre_{stim} + F_{MTC,SOL}G_{SOL} & \text{Stance} \\ Pre_{stim} & \text{Swing} \end{cases} \quad (15)$$

The parameters used for the experiments are stated in table 1.

Simulations

Before the experiment two different simulation methods were used to check the feasibility of the NMC. Both were modelled in Matlab Simulink 2014b. This led to a better insight in what could happen in the experimental set-up and with it, it is predicted that the NMC would not aid but instead augment the backward push and aids the forward push less than what would be desired. More information about the exact execution of simulations can be found in Appendix A and B.

Experiments

Subject criteria

The subjects should be older than 18 years, have no history of orthopaedic or neuromuscular impairments and can walk at a normal pace (0.7 m/s) for an hour without problems. Due to the size of the ankle exoskeleton, the shoe size must be between size 36 and 45 and the subject must be at least 1.65 m tall. An overview of the subjects is given in table 2. All subjects signed an informed consent before starting the experiment.

The setup

The setup consisted of a split belt treadmill with 6 DOFs force sensors (Motekforce Link, Amsterdam, the Netherlands), a pushing device around the hip (SMH60, Moog, Nieuw-Vennep, The Netherlands), EMG (Trigno Wireless Systems and Smart Sensors, Delsys inc., Natick, Massachusetts, USA), visualeyez to measure kinematic data (Phoenix Technologies Visualeyez, Canada) and Achilles an ankle exoskeleton [18]. See figure 6 for a better overview of the experimental set-up. The split belt treadmill was used to measure the ground reaction forces for each foot, these forces [17]. were used to determine the gait phase during the experiments and used for inversedynamics. These forces were

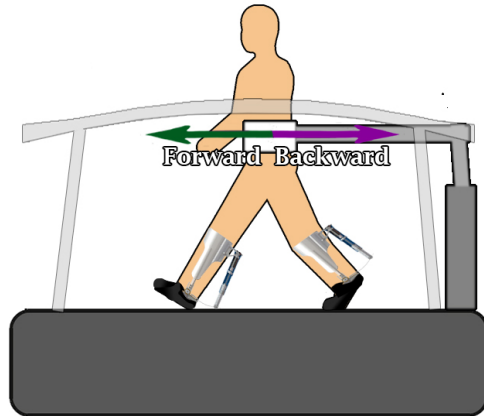


Figure 6: Setup side view, where the subject is walking on a treadmill, with the pusher attached around the hip and the Achilles worn around the ankles and lower leg.

synchronized with the visualization system Visualeyez, this system could determine the location of the body which was later used for kinematics and for inverse dynamics. The pushing device around the hip caused the disturbance. The timing of the push was determined by the gait phase obtained from the treadmill. From the Trigno Wireless System EMG data was collected which was also synchronized with the rest of the data. Lastly on the Achilles various variables were obtained of the controller output and internal workings and was synchronized with the data acquired on the other devices during the experiment. The controller was the same as used in Dzeladini et al.

Data collection

The data on the Achilles and the Visualeyez computer was collected using a frequency of 100 Hz and the data for the pusher, EMG and the split belt treadmill were collected using a sample frequency of 1000 Hz. The data was measured on three different devices and a synchronization signal was later used to synchronize all the data.

For the kinematic data the feet, shank, thigh, pelvis and trunk segments were measured on both left and right side. On each of these segments, LED-clusters were placed, additional single LEDs were placed on the knee and ankle joints. For each segment at least 3 bone structures were probed to know the exact location of the segment with correspondence to the LEDs. The EMG of the Soleus (SOL), Gastrocnemius (GAS) and Tibialis Anterior (TA) of the right and left leg were measured. The locations of the EMG was decided using seniam guidelines [21]. If the EMG location was underneath the Achilles, the location was moved to the

closest spot possible, which was still on the muscle.

Protocol

From the data driven simulation data values far exceeding the maximum capacity of the Achilles were obtained (Appendix B). The maximum output of Achilles is 50 Nm, while for a backward disturbance the NMC generates a torque of 100 Nm (Appendix B). Therefore the output of the NMC was reduced to 50% to prevent saturation. For the experiment three different conditions were tested: natural walking on a treadmill, walking on a treadmill with the Achilles with zero-impedance control and walking on a treadmill with the Achilles with NMC. For each of those conditions the following trials were performed:

- **Familiarization period** a period of 3-4 minutes of normal gait on a treadmill. Allowing the subject to get used to the condition.
- **Pushes before training** 8 pushes in forward and 8 pushes in backward direction. Every 6-12 steps a push was given in a random order. These were later compared to the pushes after the training to check if learning occurred.
- **Training** 30 pushes in forward and 30 pushes in backward direction every 2-3 steps.
- **Pushes after training** 8 pushes in forward and 8 pushes in backward direction. Every 6-12 steps a push was given in a random order. These were later compared to the first pushes of the training to check if learning occurred and were used for the rest of the data analysis.

There was a rest period of at least 3 minutes between the 3 different conditions. The speed the subject walked at was $2.27 * \sqrt{leglength}$ km/h and the pushes were at $16\%ofbodyweight * 9.81$. The pushes were consistently given at right feet toe off for 150 ms.

Variables

For the analysis the following signals were analysed:

- **EMG:** GAS, TA and SOL left leg
- **NMC for both TA and SOL and left and right leg:** Stimulation and force muscle
- **Achilles:** Measured torque
- **Body:** Left ankle angle, left ankle torque, left ankle location, right feet ground contact location, centre of mass (COM) location and COM velocity

Analysis

In the analysis all the data was synchronized and processed using Matlab 2014b. The calculations of the kinematics and inverse dynamics can be found in appendix C. All signal plots are normalized in time between the phase events: push/right toe off, right heel strike and left toe off. Additionally, the torques were normalized with the weight and leg length of the subject and step size was normalized to leg length. The EMG was first high pass filtered with 10 Hz, then rectified and low pass filtered with a 6th order 10 Hz cut off frequency, both filters were Butter-worth filters.

EMG is used to see if the muscle activity of the ankle muscles was affected by the controller. The internal controller values are used to see what caused the desired torque by the Achilles. The measured human ankle torque is used to see if the ankle strategy changes when using a controller. The COM velocity and location with respect to the left ankle location and right feet ground contact location is used to see if there is a change in balance recovery.

The data from various subjects will be averaged for all subjects together for the final results. Except for EMG, which will be looked at individually due to the difference in placement between the subjects. The statistics will be done using a Friedman test using SPSS and if a significant difference between different controllers is present this will be indicated with an '*' in the results.

3 Results

It is unknown whether a NMC gives a positive or negative contribution to balance for healthy subjects. Therefore, a simulation with a full NMC humanoid model and a data driven ankle NMC is first tested to give insight in the possible contribution of the NMC to balance recovery (Appendix A and B). From the forward simulation the responses were minimal in comparison to experiments and different from human movement (Appendix A). For the data driven simulation the response was neither the same as the human movement and was enormous compared to both the forward simulation and the human movement for the backward push (Appendix B). For the backward disturbance the output of the data driven simulation was more than twice the capacity of the Achilles. Therefore, to

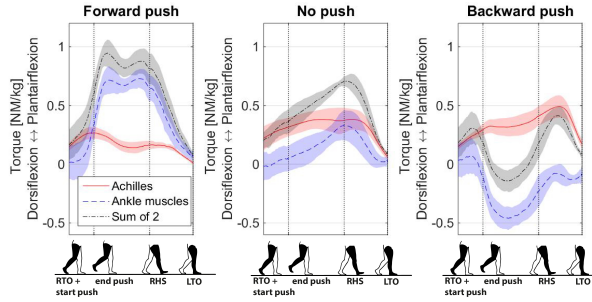


Figure 7: The total torque around the ankle, dissolved in Achilles contribution and the natural ankle contribution of muscles and ligaments. The segments are normalized in time and are indicated at the x-axis. This is only for done for the condition with the NMC.

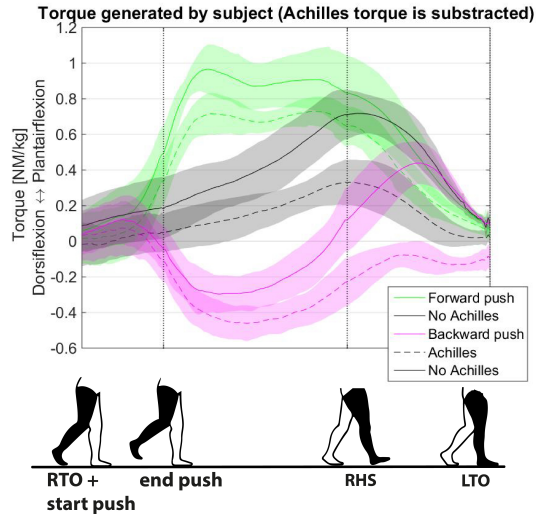


Figure 8: Contribution of ankle muscles and ligaments to torque without Achilles and with NMC for forward and backward pushes. When the NMC was active, the torque calculated by the NMC was subtracted from the total torque around the ankle resulting in the torque generated by the ankle muscles and ligaments. The segments are normalized in time and are indicated at the x-axis.

prevent extensive saturation, the exoskeleton only gave 50% of the calculated torque by the NMC, as is also stated in the Methods and Materials. The experiments were still continued as it is not known what the interaction between the human and the NMC during a disturbance will do. It is known from other research that angles change depending if there is support from an ankle exoskeleton [17, 19].

The calculated torque of the NMC during normal gait seems to corresponding to human torques generated during normal walking, for the

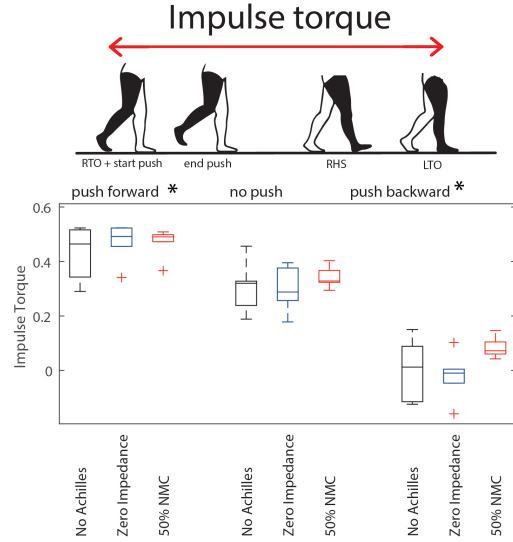


Figure 9: The impulse of the torque generated by ligaments, muscles and Achilles for all conditions. The area under the curve that was taken was from the start of the push at RTO until the LTO.

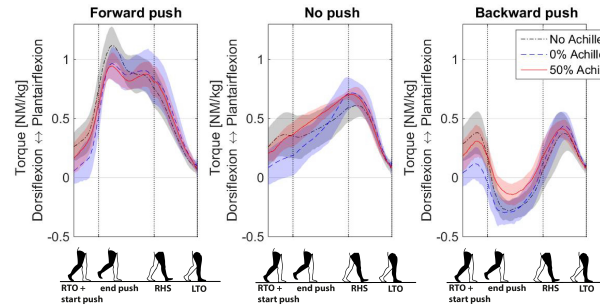


Figure 10: The total ankle torque (Achilles + muscles and ligaments) for different controllers and different disturbances, normalized in time for each segment indicated at the x-axis and normalized in weight.

disturbances this is not the case. The calculated torques from Achilles do not correspond to human torques generated during normal walking as was predicted in the simulations. After the forward push, where more plantar flexion is generated by the subject, the NMC gives less plantar flexion compared to normal gait and where dorsion flexion is needed at the backward push the NMC gives more plantar flexion (figure 7). The torque of the NMC adjusts to the disturbance, in a not relative assisting manner. When the torque generated by the NMC is subtracted from the total torque around the ankle and comparing this to the ankle torque when no Achilles is worn, it can be seen that the human always compensates for the additional plantar flexion by lowering its own plantar flexion (figure 8).

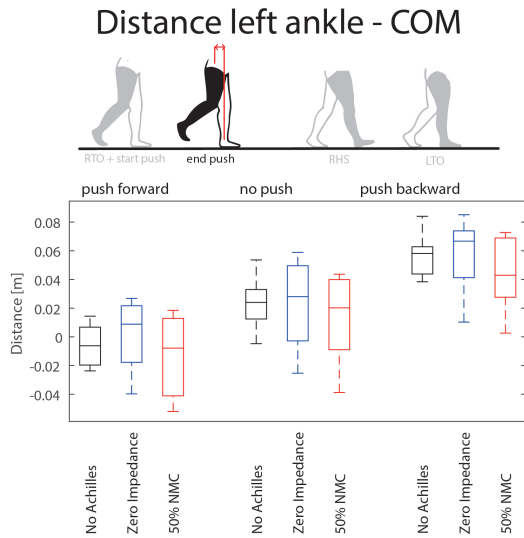


Figure 11: Distance COM and left ankle at the end of the push for different conditions, for a positive value the ankle is in front of the COM (for example at heel strike during normal gait) and for a negative value the ankle is in behind the COM (for example at toe off during normal gait).

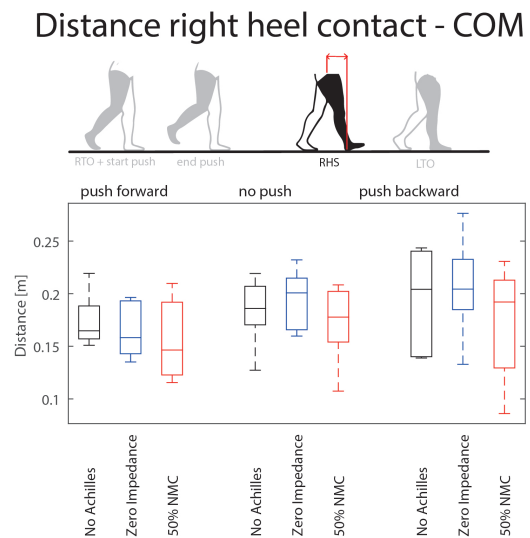


Figure 13: Distance COM and left ankle angle at RHS for different conditions, for a positive value the ankle is in front of the COM (for example at heel strike during normal gait) and for a negative value the ankle is in behind the COM (for example at toe off during normal gait).

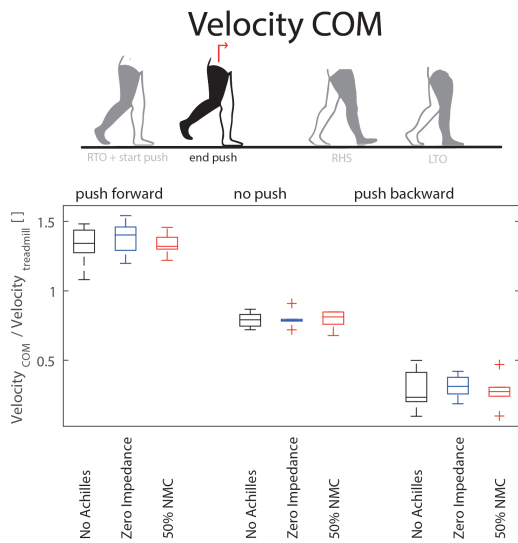


Figure 12: COM velocity direct after the push for different conditions and perturbations. A value above 1 indicates a velocity higher than the treadmill velocity and a velocity lower than 1 indicates a velocity underneath the treadmill velocity.

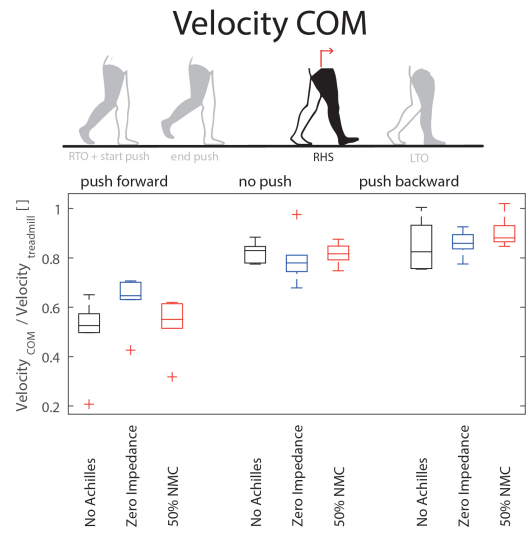


Figure 14: COM velocity at RHS for different conditions and perturbations. A value above 1 indicates a velocity higher than the treadmill velocity and a velocity lower than 1 indicates a velocity underneath the treadmill velocity.

For the impulse of the total ankle torque (Achilles + human) it appears that the variation at the NMC is less than the no achilles or zero impedance (figure 9). When looking at the pattern of the total ankle torque in figure 10, it can be seen that the torque is closer to the normal gait pattern

in both the forward and the backward push than when walking with only zero impedance control. If the additional torque is given at the right moment this could aid in balance recovery, if not this could augment the disturbance.

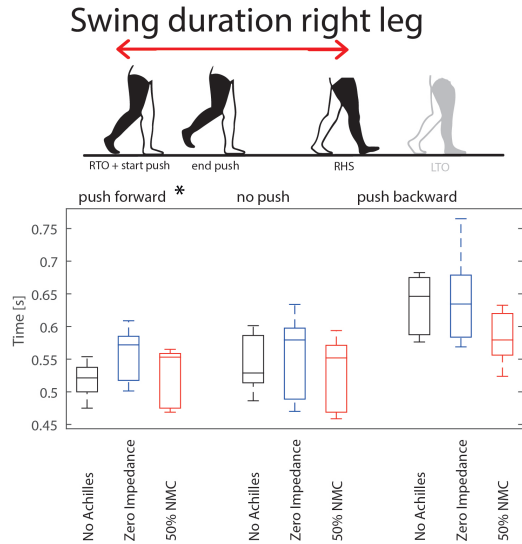


Figure 15: Swing duration right leg from push at RTO until heel contact for different conditions and perturbations.

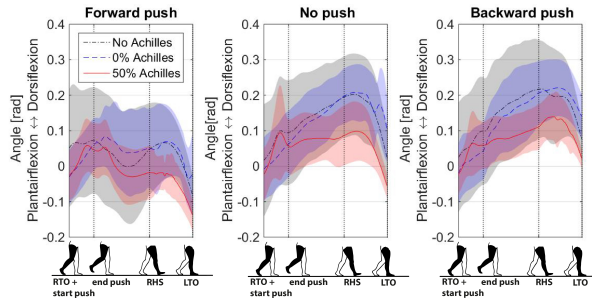


Figure 16: The ankle angle for different controllers and different disturbances, normalized in time for each segment indicated at the x-axis.

For balance recovery the moment of the added plantar flexion is important. Additional plantar flexion when the COM is not yet in front of the ankle yet could worsen balance recovery. For the backward push the ankle joint is in front of the COM directly after the push (figure 11). At this moment the ankle is responding with dorsion flexion (figure 10). Additional plantar flexion could cause the COM to slow extra down which is not wanted as the velocity of the COM has already slowed down extra compared to normal gait (figure 12). At the end of the forward push the COM is approximately above the ankle joint (figure 11). Additional plantar flexion would aid in the reduction of the forward COM velocity as long as the COM is behind the ankle joint. But the NMC gives less plantar flexion at the start compared to normal gait, and is reducing its support compared to normal gait (figure 7). However not much difference between the different controllers is expected here

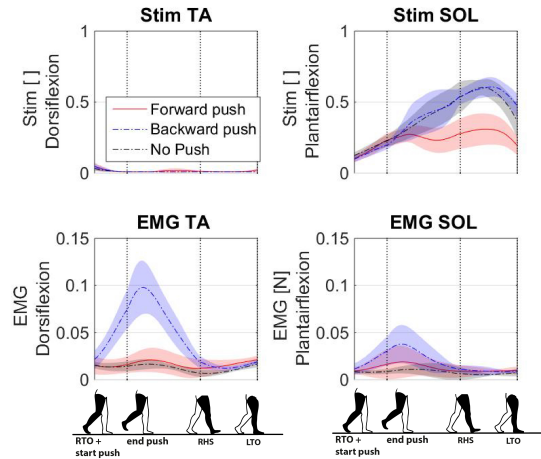


Figure 17: High lighted variables of the NMC, the stimulation and the force calculated for the muscles modelled in the NMC. The stimulation is the closest representative of EMG. The variables are normalized in time for each segment indicated at the x-axis

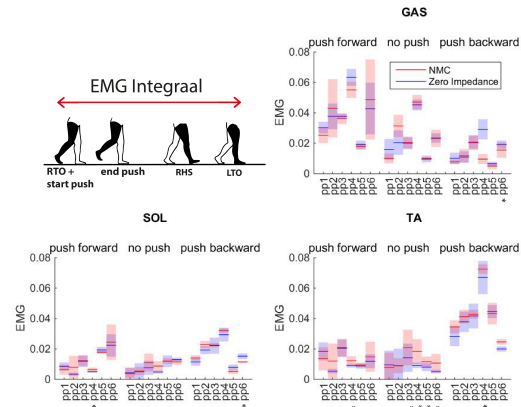


Figure 18: EMG integral for different subjects of the GAS, SOL and TA for the Zero-Impedance and the condition with NMC. The integral is taken from the start of the push at RTO until LTO.

yet as the controller has not contributed a lot to and/or against the disturbance (figure 7).

At the right heel strike the velocity of the COM seems similar to normal gait for the backward push but not for the forward push (figure 14).

This indicates that balance recovery for the forward push was more difficult, as the speed after the push was so high that during the rest of the stance phase the movement had to be significantly slow down to be able to restore balance. But, there is hardly any difference between the different controllers NMC and the normal gait, though for some reason the zero impedance is closer to the velocity of normal gait at RHS, it is unclear if this is positive or a negative.

The distance between the COM and the right heel at RHS are similar for all conditions (figure 13). Therefore no disturbances can be found here. The right swing duration seems slightly shorter for the NMC after the backward push but there is only a minor difference (figure 15).

For the ankle angles there is a big difference between the different controllers (figure 16). The biggest difference is seen between Achilles on and Achilles off. This indicates that constrains the DOF of the ankle to only plantar flexion and dorsion flexion induces a change in the ankle angle or it could indicate that the zero impedance has an influence on the behaviour of a human as it is slightly noticeable. Also between the zero impedance and the NMC differences can be found.

For the EMG only the NMC and zero impedance are compared as this tells us if the controller has an effect and not if the exoskeleton has an effect. The results are shown individually and even for individuals a lot of variation can be seen in the EMG (see figure 18). The results are highly variable and there are hardly any results significant. Indicating that with the current method no significant differences can be found between the NMC support or not.

From the EMG we can see that there is always some activation in both the SOL and the TA, the similar component in the NMC shows a different response. The neural stimulation in the NMC is zero for the TA during stance, for humans the TA is active during stance (figure 17). This means that there is a defect with the feedback loop for the neural TA activation in the NMC and could be improved.

A learning effect due to the repeated pushes was not found. There was some adaptation to the pushes, but this was during the conditions without Achilles and were quite small. Only the last pushes after the training period were used for the data analysis not the first few pushes as it was not checked if there was learning for the first 1-2 pushes but for the first 8 compared to the last 8, therefore the last 8 pushes are more reliable.

4 Discussion

The current findings indicate that the NMC needs improvements for balance recovery. This is especially needed if the controller will be used for people with SCI as they cannot depend on their own legs to recover balance and when they fall they cannot get back up. The NMC always generates a dorsal

torque and never a plantar torque. That the NMC does not generate a plantar flexion torque, is due to the inactivity of the virtual TA in the NMC. The cause of this inactivity, probably lies in the optimization method of the parameters or the neural activation in the reflex loop of the model.

The parameters for the neural activation are all decided with an optimization method. The optimization method used for this model is mainly based on two cost aspects: it may not fall and the virtual muscles should use as little energy as possible [13–15]. This does not include balance disturbances, which is tested with this experiment. This could also explain the unwanted results as the model is not optimized for this aspect. Tycho Brug [22] used another optimization method which included the cost: making the data look as close as possible to experimental data [22]. This did result in the model being closer to experimental data during normal gait. Though for disturbances this does still result in extra plantar flexion when less plantar flexion is desired and less plantar flexion when more is required (in comparison to normal gait). Even though this is only tested in a virtual environment and not in an experimental setting, it does indicate that changing the parameter set alone is not a sufficient solution.

The neural activation in the model is currently relatively simple. It is a feedback where the feedback gains and connections change depending on the phase of the gait. For the SOL and TA this means that the gain changes depending if the feet is on the ground or off the ground. During normal gait this is sufficient, though during a disturbance a different feedback is needed, as the findings imply.

An option to change the neural activation is to change the connection between the muscles. The TA activation is for example besides its own length depending on the force generated by the SOL (equation 14). This connection is assumed from normal gait but not for disturbances [15]. The SOL however is solely dependent on its own force (equation 15). A different connection seems needed during a balance disturbance. This could best be decided by changing the connection to various other connections and testing which one has the desired effect.

The NMC should respond similar to a human, the neural aspect of the controller should be closer to that of the human as well. Adding balance detection and changing the control upon the detection could make the response more similar. Using neural pathways from the legs to the brain and back takes approximately 0.09 s [23]. This means that the

brain can theoretically respond to the disturbance before the end of the push in this experiment (push duration = 0.15 s). None of this can be seen in the controller, but the experimental data implies that there is such a strategy present as the torque for the disturbances are different from normal gait. Therefore it would make sense to implement active decision making of the brain when a disturbance is detected.

The detection could be done with the velocity or acceleration of the COM. As the velocity of the COM differentiates too much from the intended gait velocity as there is a clear difference between the backward push, the forward push and normal gait at the end of the disturbance (figure 12). The horizontal distance between the stance ankle and the COM is not a good indicator as there is much overlap between the normal gait and the push forward or backward for these specific disturbances.

When disturbed, and this is detected instead of using NMC, another type of control could be used to counteract the disturbance. When the COM velocity is involuntary reduced and the COM is behind the ankle, extra dorsal flexion aids the balance recovery until the COM is before the ankle then extra plantar flexion is needed to aid balance recovery for an increased velocity the opposite strategy would apply. Instead of controlling this with NMC a temporarily imposed controller could be used to implement this strategy.

It should be noted that there is one important plantar flexion generating muscle missing in the controller, namely the GAS. The GAS is a bi-articular muscle over the knee and the ankle [5, 24]. To program the GAS the knee angle is needed, but the Achilles does not have a sensor for the knee ankle and is therefore not simulated [18]. This could have influenced the results, however the GAS is a muscle for plantar flexion and will never generate dorsal flexion [15]. Therefore the results for the backward push would not change positively and would still result in plantar flexion. However, for the normal gait and forward push it might have a positive contribution and should be modelled but more changes than just adding the GAS should be performed to get a desired response for both the backward and forward push.

Another point which should be taken into account is that the controller is speed specific and specific for a subject of 80 kg and 1.80 m. If the NMC would be implemented in controllers for person specific subjects it should be optimized for different speeds and different persons. It is known that for different velocities different parameter sets

exist [25]. It should also be possible to do this for different subject characteristics, resulting in a NMC optimized for a specific subject with variable speeds. This is a limitation of the current NMC and is solvable.

An important point is that this research is only researching two specific disturbances. It is not known if the NMC is also inappropriate for other disturbances. There has been some research with NMC and disturbances in simulations but not much could be found on similar situations in an experimental setting with an exoskeleton [11, 15, 16]. The closest are experiments on an ankle-knee prosthesis [26, 27]. In this experiment the performance of the NMC is better than other controllers. However, it was mostly tested on rough terrain and not on the specific disturbance tested in this paper [26, 27]. Furthermore, with a prosthesis on one leg and one leg without a prosthesis which still has the human control, it is a significant different situation from a situation where both legs do not work. It would be recommendable to look at balance recovery in healthy subjects and compare this to the response of the NMC in healthy subjects for a lot of other disturbances than the ones tested so far.

Besides the NMC there were some other shortcomings and/or unknowns in the research. It is not known what effect a treadmill has on balance recovery. Therefore it would be good to research if there is a difference between balance recovery when walking overground and when walking on a treadmill. Another problem would be the force restriction of the Achilles. The Achilles does simply not deliver enough force to be able to completely support the torques around the ankle during normal gait, let alone disturbances. Therefore an exoskeleton around the ankles with at least 100Nm plantar and dorsion flexion is needed. If the exoskeleton has to be changed (due to the torque limitation), it would also be good if the exoskeleton is not covering skin where EMG for muscles should be placed. This is not a problem when no EMG is required. Furthermore the Achilles is not very adjustable for different subjects. It is not known what effect this has on the measured variables, though not much difference is expected but should still be tested in an experimental setting. Lastly the number of participants in this study is relatively low and not very variable. It is known that different genders, ages and different ethnicities can influence the results [28]. To get clearer results more subjects and more variations between subjects are recommended.

The variables: Velocity COM, swing duration right leg, distance right heel contact - COM, im-

pulse total torque and distance left ankle - COM do not show a large difference between different controllers. This is not surprising as the total torque around the ankle is not changing too much between different controllers. However, these variables can help us getting a better understanding in balance recovery. The velocity of the COM is for example highly affected at the end of the push, with no overlap with either the opposite push or normal gait. At RHS the velocity of the COM is already somewhat restored the values of normal gait. Similar responses are also found in Vlutters et al. [29], which has the same set-up as this research without the addition of the ankle exoskeleton and was therefore successfully reconstructed with a slight addition.

For the EMG we would expect that for the normal gait and the forward push the EMG of the SOL and or GAS would reduce for the NMC, while for the backward push we would expect the TA to have extra activation. Unfortunately this is not seen in the results as there is not much difference and/or no consistency between subjects. A similar result is seen in Dzeladini et al. [17], where the response in EMG is different between subjects with only a small difference between situations. Unfortunately in Dzeladini et al. [17] no standard deviations are shown making it unclear if the differences are significant. A possible cause could be that most of the activation of the ankle muscles are used for stabilizing the joint and the addition of the NMC does only cause a tiny difference in the EMG signal. Another option would be that the other muscles are causing the torque changes. Unfortunately those cannot be measured with superficial EMG as other muscles lay over those muscles. The last and most probable cause would be that the additional support is too small, causing the not change enough in comparison to the deviation.

For the TA EMG we can see a significant rise in 4 of the 6 subjects, this could indicate that instead of reducing the workload of the plantar flexors the dorsi flexors increases. This is not energetically favourable therefore this result is strange. A reason for the extra dorsi flexion when there is a supportive plantar flexion could be to increase the stiffness of the ankle and with it increasing stability. It is strange that this effect is not seen back in the disturbances.

The torques found for the disturbances without Achilles are comparable to those found in Vlutters et al. [20]. When adding the NMC the human body responds by compensating for the added torque, keeping the same torques as found for the disturbances and normal gait without NMC.

Though the ankle angles do change as also happens without disturbances in Dzeladini et al. [17]. This means that it is more important for human gait to sustain the torque around the ankles than the ankle angle. Unfortunately there was no information on knee or ankle angles to check if the difference in ankle angles are countered by those joints or somewhere else. This is indicated as there is no difference in horizontal distance between the ankle and COM for different controllers what is just as the ankle angle a measure of position and therefore some of the changes in the ankle angles would be expected to be reflected in this variable.

5 Conclusion

The results of the experiments tell us that the current controller is not sufficient for balance recovery for the tested disturbances. The results of the experiments reflect the torque results from the data driven simulation though they are less extreme due to the added interaction between human and controller. In the experiments the addition of the NMC to balance recovery during gait mostly changed the torque generated by the muscle and ligaments, though the total amount of torque around the ankle stays approximately the same. Therefore there is not much differences between conditions for other variables that could indicate balance (recovery). However a healthy subject can adjust to the force delivered by the Achilles, a SCI subject cannot adjust the perpendicular response of the NMC. For them the NMC will augment the disturbance instead of aiding balance recovery after the backward push. Even though in the simulation, the humanoid can keep walking, it is still not set in stone that this will also apply for reality. If the NMC will be used in a clinical setting or even for daily use of SCI patients, then the controller must be absolutely reliable. Therefore a response similar to a human is preferred and the current NMC should change its response to this specific disturbance. Lastly, there is no learning difference between the first 8 pushes and the last 8 pushes with a training of 30 pushes for this disturbance. This does not exclude learning completely as learning could occur very fast or very slow, however this was not tested.

6 Recommendations

There are several approaches of changing the NMC. As the NMC does seem promising for regular gait

[17], it would only need an appropriate response to disturbances securing the safety of the impaired subject. If only this disturbance is not properly absorbed then a detection of the disturbance and a temporarily different control would be in its place. This does not necessarily have to be NMC, as the main objective would be to regain balance and normal gait. This would only be a minor change to the whole controller.

This research does not exclude that for other responses the NMC does have an inappropriate response. It could be recommended to look at more types of disturbances during gait. Depending on the other disturbances it could then be decided how to change the controller. Data from these disturbances, either experimental or simulation data, could lead to a better parameters set of the NMC for the optimization.

If there is a sufficient amount of disturbances which are not properly absorbed then a change of the controller should be considered. The NMC itself could be changed either only in parameters set or even in its structure. Especially the neural system is still quite simple and a lot of improvement could be done in that area.

As the NMC is now, it is better not to use the NMC for daily life use of a SCI patient, as safety cannot be guaranteed. It is not known yet how the NMC responds to all kind of disturbances and as the controller does not respond appropriate for the disturbances in this paper this should first be solved. If the response of the NMC is similar to what a healthy subject does it would then be recommended to test and possibly use it for SCI patients.

References

- [1] William J Kraemer, Steven J Fleck, and Michael R Deschenes. *Exercise physiology: integrating theory and application*. Lippincott Williams & Wilkins, 2011.
- [2] <https://basicmedicalkey.com/lower-limb-2/>. Seen at 24 July 2017.
- [3] M. Wyndaele and J.-J. Wyndaele. Incidence, prevalence and epidemiology of spinal cord injury: What learns a worldwide literature survey? *Spinal Cord*, 44(9):523–529, 2006.
- [4] J.W. Middleton, A. Dayton, J. Walsh, S.B. Rutkowski, G. Leong, and S. Duong. Life expectancy after spinal cord injury: A 50-year study. *Spinal Cord*, 50(11):803–811, 2012.
- [5] K. Hoehn E.N.Marieb. *Human Anatomy and Physiology eighth edition*. Pearson Education Limited, 2010.
- [6] R. Van Den Brand, J. Heutschi, Q. Barraud, J. DiGiovanna, K. Bartholdi, M. Huerlimann, L. Friedli, I. Vollenweider, E.M. Moraud, S. Duis, N. Dominici, S. Micera, P. Musienko, and G. Courtine. Restoring voluntary control of locomotion after paralyzing spinal cord injury. *Science*, 336(6085):1182–1185, 2012.
- [7] Khairul Anam and Adel Ali Al-Jumaily. Active exoskeleton control systems: State of the art. *Procedia Engineering*, 41:988 – 994, 2012. International Symposium on Robotics and Intelligent Sensors 2012 (IRIS 2012).
- [8] M.R. Tucker, J. Olivier, A. Pagel, H. Bleuler, M. Bouri, O. Lamercy, J.R. Del Milln, R. Riener, H. Vallery, and R. Gassert. Control strategies for active lower extremity prosthetics and orthotics: A review. *Journal of NeuroEngineering and Rehabilitation*, 12(1), 2015.
- [9] T. Yan, M. Cempini, C.M. Oddo, and N. Vitiello. Review of assistive strategies in powered lower-limb orthoses and exoskeletons. *Robotics and Autonomous Systems*, 64:120–136, 2015.
- [10] R. Jimnez-Fabin and O. Verlinden. Review of control algorithms for robotic ankle systems in lower-limb orthoses, prostheses, and exoskeletons. *Medical Engineering and Physics*, 34(4):397–408, 2012.
- [11] S.A. Haghpanah, F. Farahmand, and H. Zohoor. Modular neuromuscular control of human locomotion by central pattern generator. *Journal of Biomechanics*, 2017.

- [12] A. V. Hill. The heat of shortening and the dynamic constants of muscle. *Proceedings of the Royal Society of London B: Biological Sciences*, 126(843):136–195, 1938.
- [13] M.F. Eilenberg, H. Geyer, and H. Herr. Control of a powered ankle-foot prosthesis based on a neuromuscular model. *IEEE Transactions on Neural Systems and Rehabilitation Engineering*, 18(2):164–173, 2010.
- [14] H. Geyer and H. Herr. A muscle-reflex model that encodes principles of legged mechanics produces human walking dynamics and muscle activities. *IEEE Transactions on Neural Systems and Rehabilitation Engineering*, 18(3):263–273, 2010.
- [15] Seungmoon Song and Hartmut Geyer. A neural circuitry that emphasizes spinal feedback generates diverse behaviours of human locomotion. *The Journal of Physiology*, 593(16):3493–3511, 2015.
- [16] T. Geijtenbeek, M. Van De Panne, and A.F. Van Der Stappen. Flexible muscle-based locomotion for bipedal creatures. *ACM Transactions on Graphics*, 32(6), 2013.
- [17] F. Dzeladini, A.R. Wu, D. Renjewski, A. Arami, E. Burdet, E. Van Asseldonk, H. Van Der Kooij, and A.J. Ijspeert. Effects of a neuromuscular controller on a powered ankle exoskeleton during human walking. volume 2016-July, pages 617–622, 2016.
- [18] C. Meijneke, W. van Dijk, and H. van der Kooij. Achilles: An autonomous lightweight ankle exoskeleton to provide push-off power. In *5th IEEE RAS/EMBS International Conference on Biomedical Robotics and Biomechatronics*, pages 918–923, Aug 2014.
- [19] P.-C. Kao, C.L. Lewis, and D.P. Ferris. Joint kinetic response during unexpectedly reduced plantar flexor torque provided by a robotic ankle exoskeleton during walking. *Journal of Biomechanics*, 43(7):1401–1407, 2010.
- [20] H. van der Kooij M. Vlutters, E.H.F. van Asseldonk. *Joint-level responses to pelvis perturbation during human walking*. Lab of Biomechanical Engineering, University of Twente, The Netherlands, jun 2017.
- [21] Hermie J Hermens, Bart Freriks, Roberto Merletti, Dick Stegeman, Joleen Blok, Günter Rau, Cathy Disselhorst-Klug, and Göran Hägg. European recommendations for surface electromyography. *Roessingh research and development*, 8(2):13–54, 1999.
- [22] T.Brug. *Enhancing and integrating a 3D reflex-based neuromuscular model into the control of active lower-extremity gait-assistive devices*. Department of Biomechanical Engineering University of Twente, jun 2017.
- [23] Michael P. Schenk A. Arturo Leis. *Atlas of Nerve Conduction Studies and Electromyography*. OUP USA,, 2013.
- [24] W.Platzer. *Sesam atlas van de anatomie 1 Het bewegingsapparaat*. ThiemeMeulenhoff bv, 2009.
- [25] S. Song and H. Geyer. Regulating speed in a neuromuscular human running model. volume 2015-December, pages 217–222, 2015.
- [26] N. Thatte and H. Geyer. Towards local reflexive control of a powered transfemoral prosthesis for robust amputee push and trip recovery. pages 2069–2074, 2014.
- [27] N. Thatte and H. Geyer. Toward balance recovery with leg prostheses using neuromuscular model control. *IEEE Transactions on Biomedical Engineering*, 63(5):904–913, 2016.
- [28] J. Yu and K. Moeller. Investigating multimodal displays: Reaction times to visual and tactile modality stimuli. volume 43, pages 480–483, 2014.
- [29] M. Vlutters, E.H.F. Van Asseldonk, and H. Van Der Kooij. Center of mass velocity-based predictions in balance recovery following pelvis perturbations during human walking. *Journal of Experimental Biology*, 219(10):1514–1523, 2016.
- [30] D.A. Winter. *Biomechanics and Motor Control of Human Movement: Fourth Edition*. 2009.

Appendices

A Push simulations Geyer & Song’s Model compared to experimental data

Introduction

Before the Neuromuscular controller (NMC) is experimentally tested on disturbances, a simulation to get a better insight in the response is in it’s place. Therefore the forward simulation model of Geyer & Song [15] is used to gain insight on the possible response to balance disturbance during the experiments.

A disturbance around the hip is modelled in the model of Geyer & Song. This push should cause an initial response from the model. It was expected that this response will be similar to a human response and the model will keep walking. The human response data will come from experimental data of Vlutters et al. [20].

Methods and materials

For the simulation, the Simulink biomechanical human like model, controlled with a NMC developed by Geyer and Song [15] will be altered by adding a push. Outcome variables from the altered model will be used to predict the response of the Achilles (ankle exoskeleton in the experiments). All simulations will be done in MATLAB Simulink/SimMechanics environment (R2014b) with the ode15s solver.

To represent the push from the actual set-up in the Simulink model, a body actuator is added to the head-arms-trunk biomechanical segment (HAT) on a similar location as the experimental set-up, see figure 19. The push will be given at a height of 12.5% of the HAT segment in anterior and posterior direction with respect to the HAT segment. It is given at the start of the left single support stance for 150 ms with varying forces of 0%, 4%, 8% and 16% of the total body weight of a 80 kg subject. However as the response to the disturbance was small, only the push at 16% body weight is shown in the results. The model walks with an average velocity of 1.14 m/s [15]. Additionally, there are two gait pattern choices in the model, robust gait and normal gait. As there is mostly saturation of the muscle stimulation in the model for the robust gait, the normal gait pattern will be used.

For the analysis the following outcome signals will be used: The torque around the hip, knee

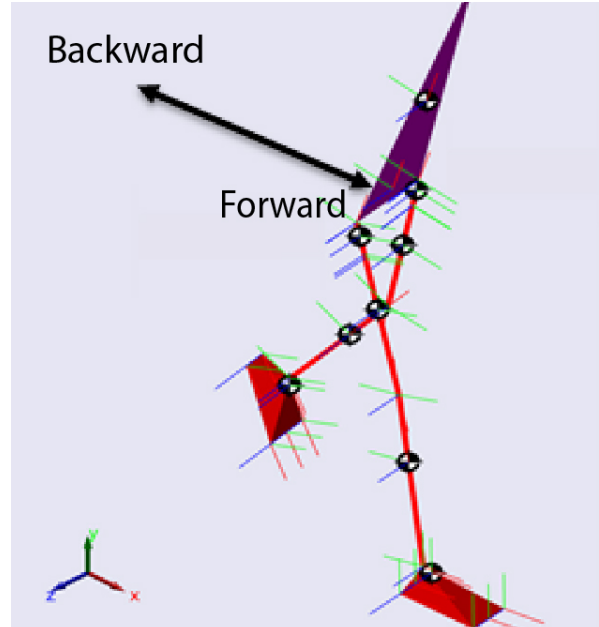


Figure 19: Location of the push in the NMC model of Geyer indicated with the black arrow at 12.5% of the HAT segment. Backward and forward indicates the direction of the pushes as the arrow implies.

and ankle; the activation, muscle force, force velocity relation of the contractile element (F_v), force length relation of the contractile element (F_l) of the Gastrocnemius (GAS), Tibialis anterior (TA) and Soleus (SOL); and the angle and angle velocity of the ankle. These signals will be compared to experimentally obtained signals like EMG and ankle torque data where a control subject is pushed at the hip with a force off 0%, 4%, 8%, 12% and 16% of the total body mass for 150 ms at the start of the left single support phase [20]. The subject walks with an approximate velocity of 1 m/s [20]. Using this, we observe whether the model uses human like responses to counteract perturbations. All of the data is normalized in time for the duration of the push, between the end of the push and the right heel strike (RHS or HSR) and between the RHS and the left toe off (LTO or LOT).

The sensitivity of the system to delays and proportional gains will also be analysed. For the sensitivity analysis, only the torque of the left ankle will be analysed as here the first response is expected to

the perturbation as the left feet is on the ground. The longest delay in the system and the gains for the proportional control of the TA, SOL and GAS will be analysed. The longest delay will be changed from 0.03 ms to 0.04 ms and 0.001 s. The gains for all muscles will simultaneously be multiplied by 0.95, 1 and 1.05. These gains were chosen after testing for which values the biomechanical simulation was still capable of 10 seconds of gait without disturbances.

Geyer & Song's model highlighted formula's

The model uses muscle and neural properties to calculate the muscle force. This section gives a better understanding of how the properties are modelled and how these are used for the analysis. For a full overview of the model it is recommended to look at the Method and Materials of the main part of the report.

The muscle force is calculated as follows [14]:

$$F_m = F_{se}(l_{se}) = F_{ce}(l_{ce}, v_{ce}, A) + F_{pe}(l_{ce}) - F_{be}(l_{se}) \quad (16)$$

Where F_m is the individual muscle force, which is in series with the tendon (F_{se}). The F_{se} can be calculated with the contractile element force F_{ce} and a combination of linear properties which limits the muscle length (F_{pe} and F_{be}). A schematic view can be seen in figure 20. From the forces who generate the total muscle tendon force, the F_{ce} element is the 'active' element and the other two are passive. The F_{ce} element is the active element as this is the only element which is directly controlled by the neural part of the system, that changes depending on the phase of the gait circle. The passive elements are modelled as springs only depending on the length of the active F_{ce} element.

The active element F_{ce} is similar to the myofibrils in muscles [5]. They have a few properties, it is activated by the neural system and has a maximum torque the muscle can generate. Depending on the length the muscle can give more or less maximum force. The velocity at which the muscle length is changing also influences the force the muscle can generate. The equation of the F_{ce} is as follow [14]:

$$F_{ce} = A \cdot F_{max} \cdot F_l(l_{ce}) \cdot F_v(v_{ce}) \quad (17)$$

Where A is the activation of the muscle (most similar to EMG), F_{max} is the maximum force of the muscle [N], $F_l(l_{ce})$ is the force-length relation of the muscle, where l_{ce} is the length of the contractile element (CE) and $F_v(v_{ce})$ is the force-velocity relation of the muscle (figure 21), where v_{ce} is the velocity that the length of the CE is changing (figure 22).

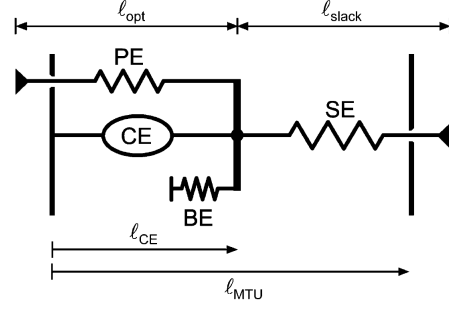


Figure 20: A schematic sketch of the muscle [13]. Where the CE is the active part of the muscle and the PE and BE are elastic buffers. The SE is similar to a tendon and is in series with the muscle.

Force-velocity curve of a muscle

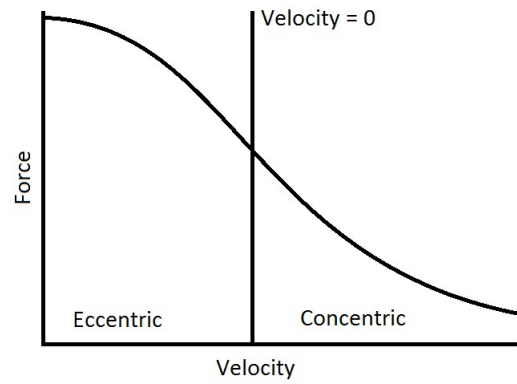


Figure 21: A schematic sketch of the F_v curve. Originating from the Hills muscle model [12], depending on an eccentric or concentric velocity of the muscle the muscle is able to generate more or less power in comparison to a velocity of 0.

Force length curve of a muscle

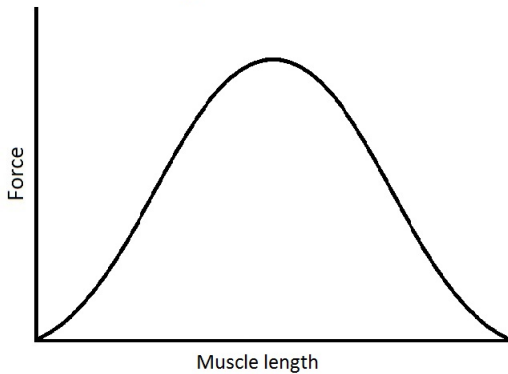


Figure 22: A schematic sketch of the F_l curve used in the NMC. Originating from the Hills muscle model [12], depending on the muscle length. If an optimum of actin and myosin elements are capable of movement in correspondence with each other more or less torque production is possible.

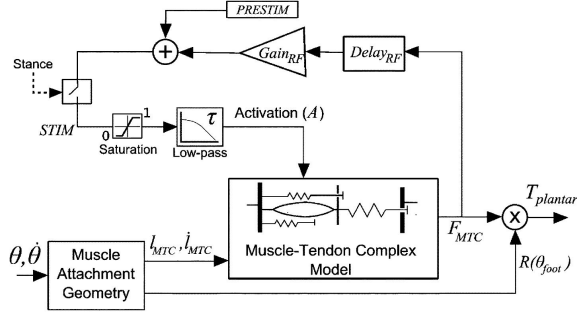


Figure 23: A scheme of the NMC for one muscle [14]. Take note that the scheme is a general scheme and between different muscles slight differences can occur in the structure. In the scheme is a representation of various parts of the muscle torque calculation namely: Muscle Attachment Geometry, Muscle-Tendon Complex Model and the activation.

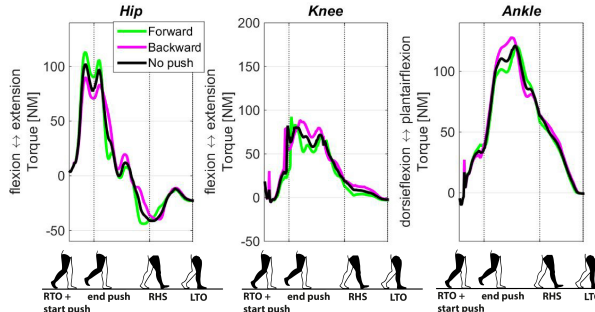


Figure 24: Torques of the left hip, left knee and left ankle in Nm after the push at right feet toe. They are normalized in time with the corresponding phases below the graph.

The l_{ce} is dependent on the total MTC length and the length of the passive element SE, see the following equation 18:

$$l_{mtc} = l_{ce} + l_{se} \quad (18)$$

The total length of the MTC depends on the angle of the joint(s) and muscle attachments. As the CE and SE elements are in series with each other both will change in length if the other changes. Though only one can actively change its length due to the activation from the neural network. Due to the pull generated from these two elements a torque will be generated on the virtual joints. This will influence the ankle angle and with it the length of the MTC, this is a closed loop. In figure 23 a scheme of this loop can be seen.

Results

The simulations should give us a good indication of the response in the experiments. However from torques of the hip knee and ankle joint only minor

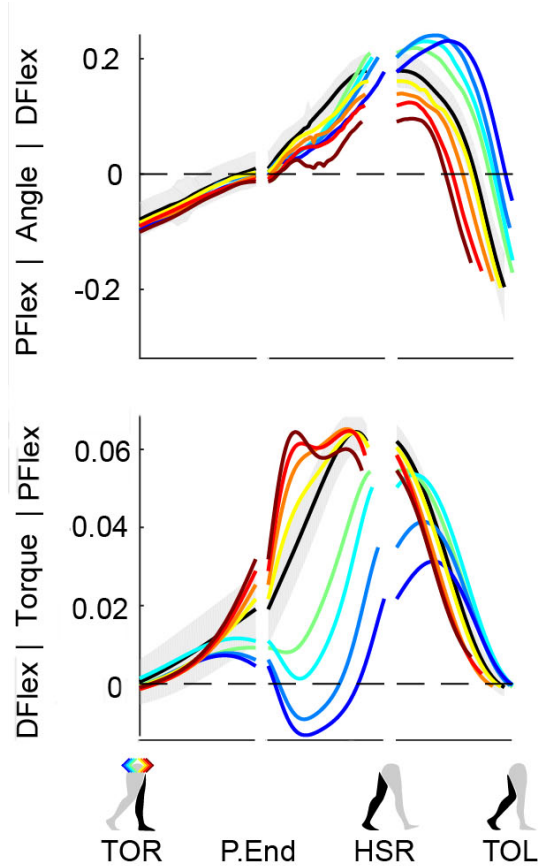


Figure 25: Torque and angle of the left ankle after push at right feet toe off (experimental data), cold colors are for the posterior pushes, warm colors are for the anterior pushes [20]. The darkest colors correspond to the pushes with 16% body weight. They are normalized in time with the corresponding phases below the graph.

responses can be seen, while in Vlutters et al. [20] much larger torques can be observed. Especially for the backward push around the ankle where the torque is even in the opposite direction for the simulations in comparison to the experiments (figure 24 and 25). This is also the torque that we are most interested in for the experiments, therefore we will focus on the ankle torque from here.

Between the forward push, backward push and normal gait, small differences for the ankle torque and ankle angle can be observed for the NMC (figure 26). From experimental data with similar disturbances, there are much larger differences observed (figure 25). This means that the response of the forward simulation to a disturbance is much smaller compared to human data. The responses are relative to normal gait not in the same direction. If the human is pushed forward the NMC gives a less plantar flexion while the human gives

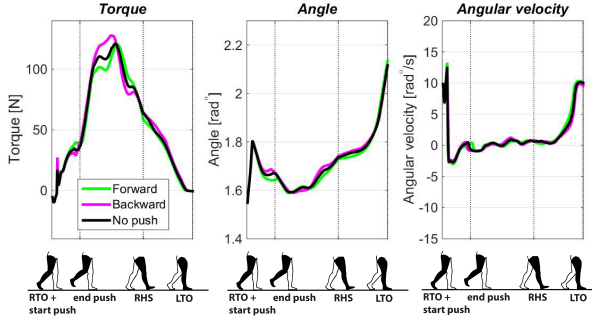


Figure 26: The simulated ankle torque, ankle angle and ankle angular velocity after the push at right feet toe. They are normalized in time with the corresponding phases below the graph.

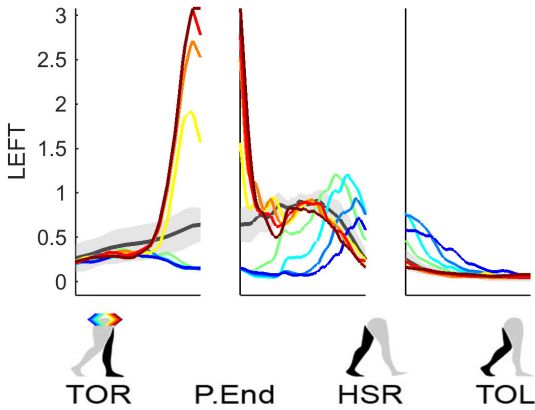


Figure 27: Activation of the GAS medial of the left after push, cold colors are for the posterior pushes, warm colors are for the anterior pushes (experimental data) [20]. The darkest colors correspond to the pushes with 16% body weight. They are normalized in time with the corresponding phases below the graph.

more. For the backward push the NMC gives more plantar flexion while dorsi flexion is observed from the human data. This means that the NMC gives an opposite reaction of a human, in the experiments this could cause for problems.

Another difference between the NMC simulation and the experimental data is the ankle angle (figure 25 and 26). The ankle angle is the input of the NMC and calculates the torque provided by the NMC. If the ankle angle in experiments with NMC on an ankle exoskeleton is significantly different from the simulations, the output of the NMC will also significantly change. Therefore this simulation might not give a good insight in the response of the NMC on healthy subjects as ankle angles in

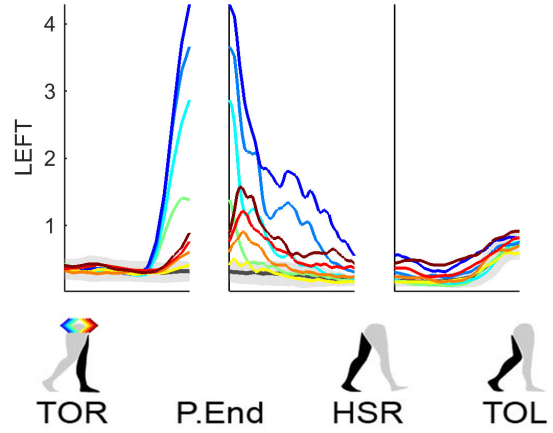


Figure 28: Activation of the TA of the left leg after push, cold colors are for the posterior pushes, warm colors are for the anterior pushes (experimental data)[20]. The darkest colors correspond to the pushes with 16% body weight. They are normalized in time with the corresponding phases below the graph.

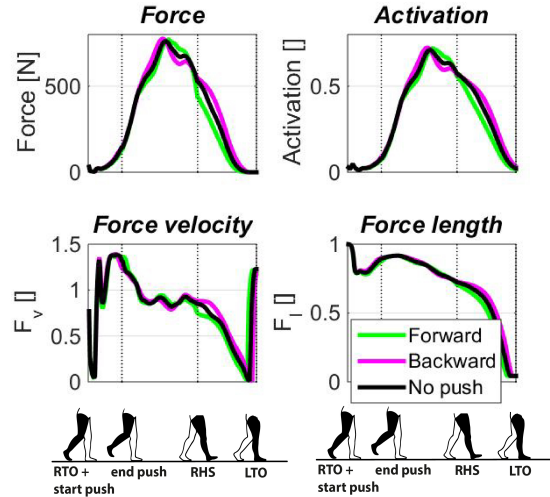


Figure 29: The F , A , F_v and F_l of the left GAS generated by the internal workings of the NMC. The variables are time normalized for each segment indicated at the x-axis.

the forward simulation and real experiments with NMC might give different results.

In the experiments from Vlutters et al. [20] an EMG response from the TA is present after the disturbances, this is not found back in the forward simulation data (figure 28 and 30). As the TA does not activate this could explain the lack of dorsal flexion for the backward push, but not the decrease in torque for the forward push. This can be seen from the activation of the Soleus. In the Vlutters et

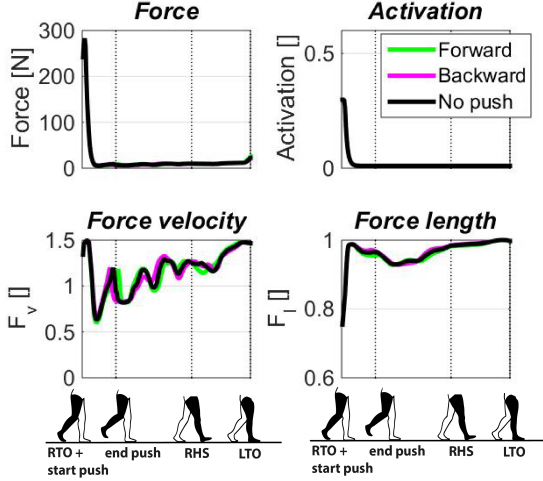


Figure 30: The F , A , F_v and F_l of the left TA generated by the internal workings of the NMC. The variables are time normalized for each segment indicated at the x-axis.

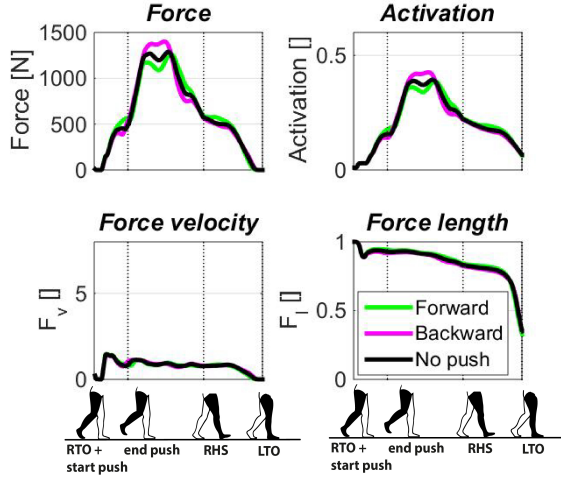


Figure 31: The F , A , F_v and F_l of the left SOL generated by the internal workings of the NMC. The variables are time normalized for each segment indicated at the x-axis.

al.[20] data initial additional GAS activation can be observed (figure 27), while less GAS and SOL activation is observed in the forward simulation (figure 29 and 31). The opposite happens for the backward push. This could explain why the response from the forward simulation is different from the experimental data of Vlutters et al. [20].

Sensitivity analysis results

The results of the sensitivity analysis show that changing either the longest delays or all the gains for all the muscles does not change the initial response to the push, see figure 32 and 33.

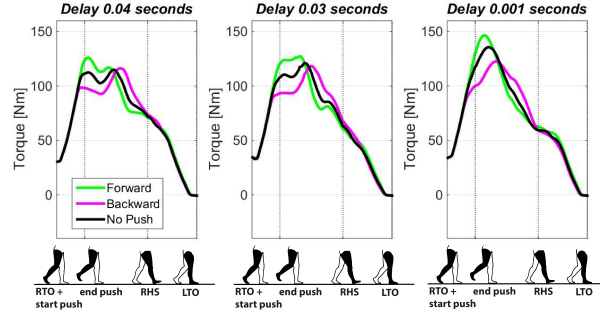


Figure 32: Sensitivity analysis ankle torques [N/kg/m/g] with different delay's of 0.04 s, 0.03 s and 0.001 s are displayed. The variables are time normalized for each segment indicated at the x-axis.

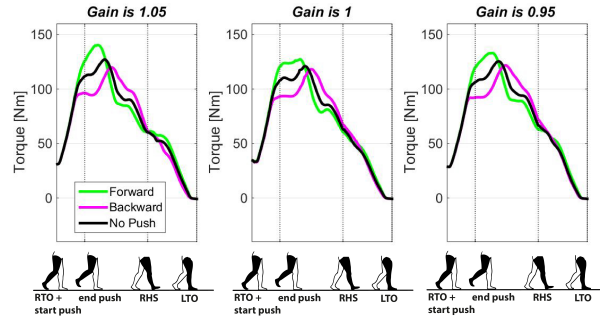


Figure 33: Sensitivity analysis ankle torques [N/kg/m/g] with different gains of 0.95, 1 and 1.05 are displayed. The variables are time normalized for each segment indicated at the x-axis.

Discussion & conclusions

From the forward simulation a small response perpendicular to the human response could be observed, though the simulated response was very small. This implies that in the simulation the controller does not correct around the ankle for a disturbance around the hip, while the human does. This strategy is most likely not favourable for balance recovery.

The angles during the experiments of Vlutters et al. [20] are different from the simulation. As the angle of the ankle joint is the input of the NMC, the response of the NMC could be very different in an experimental setting compared to the simulation. As the ankle angle will likely change to similar angles as in Vlutters et al. [20] in the experiments, a data driven simulation with data of Vlutters et al. is needed to get a better insight in the response of the NMC to disturbances.

Looking at the EMG of the human and the activation in the simulation, differences can be observed here as well. They are again not supportive of each

other and could be an indication of the need to improve the controller by changing the neural control to a similar way as a human does.

There are a few differences between simulations and real life, but the most important ones for this model are now summarized. These differences between real life and the simulations could be a cause of the differences between the data from Vlutters et al. [20] and the simulated data. The main problems are that the biomechanical model in the simulation is still a discontinuous model in a virtual environment and therefore errors can occur which are not similar to a continuous human environment. Secondly, in the simulation between the human and the controller there is no noise, in real life there will always be a form of noise. Another big problem is that the conditions in the simulation are always the same unless you change some parameters, for hu-

mans the environment and responses changes continuously. Lastly, the controller in the simulation has a not predefined number of time steps and can become much smaller than 0.001 s, while for control situation a step size is fixed at 0.001 s. A fixed step size could result in a less stable situation as the controller can respond in a smaller time frame.

As the simulation was only used to get an insight in the response of the controller for the experiments with an ankle exoskeleton with NMC, the simulation was not changed. However for further research the forward simulation should be changed to get a better prediction of disturbances applied to the biomechanical model. Furthermore, as the ankle angle of the forward simulation and the ankle angle from the experiments are significantly different, a data driven simulation is recommended.

B Data driven push simulation

Introduction

In appendix A a forward simulation of the response of the neuromuscular model is done. However the response was minimal compared to experimental data [20]. The ankle angle was also different in the simulations compared to the experimental angle. As the ankle is the input of the NMC and is important for determining the torque delivered by the NMC. A data driven simulation is used to give a better estimation of the response of the NMC when used by a healthy subject. A similar response as in the forward simulation is expected with minor changes.

Methods and materials

For the data driven simulation the same controller as in the experiments with the ankle exoskeleton will be used. This controller is from Dzeladini et al. [17]. The input of the NMC will be the ankle angle data from a single subject from the experimental data of Vlutters et al. [20].

For the analysis, the focus will be on it's output, the torque, provided by the NMC for the forward and backward push of 16% body weight and the normal gait input. These will be compared to the torques from the experimental data of Vlutters et al. [20].

Results

In figure 34 the responses are much bigger with correspondence to the data in figure 26 from appendix A. The response of the NMC is still opposite of the experimental data (figure 34). The plantar torque calculated for the backward push is almost doubling instead of becoming dorsi flexion. For the forward push the response is less compared to normal gait what is neither wanted.

Discussion & conclusion

The most important result of the data driven simulation was the huge response of the controller with the backward push. The calculated torque is far above the capacity of the ankle exoskeleton used for the experiments. The biggest downside of the data driven simulation was that there was no interaction between the response of the ankle exoskeleton and the change in ankle angle. From other research it is known that this could have a high influence on the ankle angle as this is the input of the model this could highly influence the result [17, 19].

The actual interaction between the human and

the NMC is not present in this data driven simulation, neither the interaction with the NMC if a forward or backward perturbation occurs. As the response of the NMC is most likely opposite of what the human does to the perturbations, it needs to be researched how the human interacts with this torque around the ankles. It is interesting what it will do on balance recovery, especially for the backward perturbation as the response of the NMC might augment the disturbance instead of aiding balance recovery (The NMC generates plantar flexion instead of dorsal flexion which is generated by the human).

Furthermore, there was no documentation of ankle NMC on an exoskeleton and disturbances to my knowledge. Therefore the experiments were necessary to gain an insight in the balance recovery on healthy subjects with ankle NMC on an exoskeleton. This experiment could also give an insight in the response of humans to a support perpendicular to what they would do.

Recommendations

As the data driven simulation and the simulation from appendix A both indicate that the response of the torque data from the NMC is different from the experimental data, there is a chance that the NMC changes the balance recovery. Also the ankle angle, which is the input of the NMC, will most likely change due to the support. Therefore it is not clear what will happen to the output of the NMC and the response of the subject and is still interesting even if the support to disturbances will most likely be unusable for impaired subjects. As the torque calculated by the NMC is approximately double that of the Achilles (ankle exoskeleton) [18] the output of the NMC is recommended to be put at 50%.

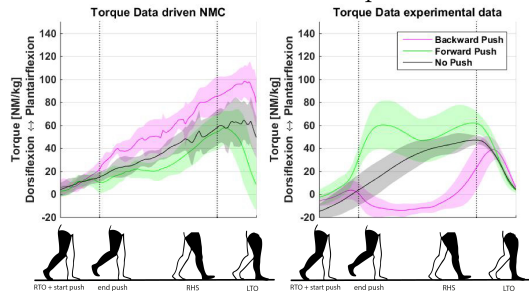


Figure 34: Torque output of the data driven NMC in comparison with the torque calculated in the experimental data. The data is from a single subject and the ankle angle used for the data driven torque of the NMC is from the corresponding data set of the experimental torque data.

C Calculation of inverse dynamics

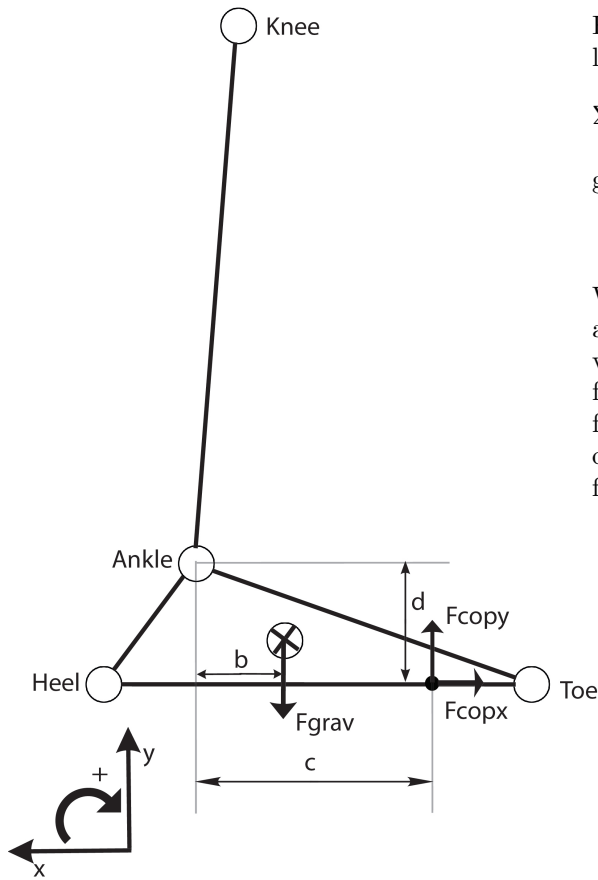


Figure 35: Schematic sketch of the ankle for the inverse dynamic calculation of the ankle torque, with an indication of the axis.

For the calculation of the ankle the following equilibrium equations for the torque:

$$\Sigma T_{ankle} = T_{ankle} + b \cdot F_{grav} + c \cdot F_{copy} + d \cdot F_{copx} = I \cdot \omega \quad (19)$$

gives:

$$T_{ankle} = -b \cdot F_{grav} - c \cdot F_{copy} - d \cdot F_{copx} + I \cdot \omega \quad (20)$$

With T_{ankle} as the torque around the ankle, F_{grav} as the gravitational force of the foot, F_{copy} as the vertical force from the COP, F_{copx} as the horizontal force of the COP, I is the moment of inertia of the feet, calculated with values gained from the book of Winters [30] and ω is the angular velocity (see figure 35).

D Additional figures

Figures of the comparison of the 8 pushes before and 8 pushes after training.

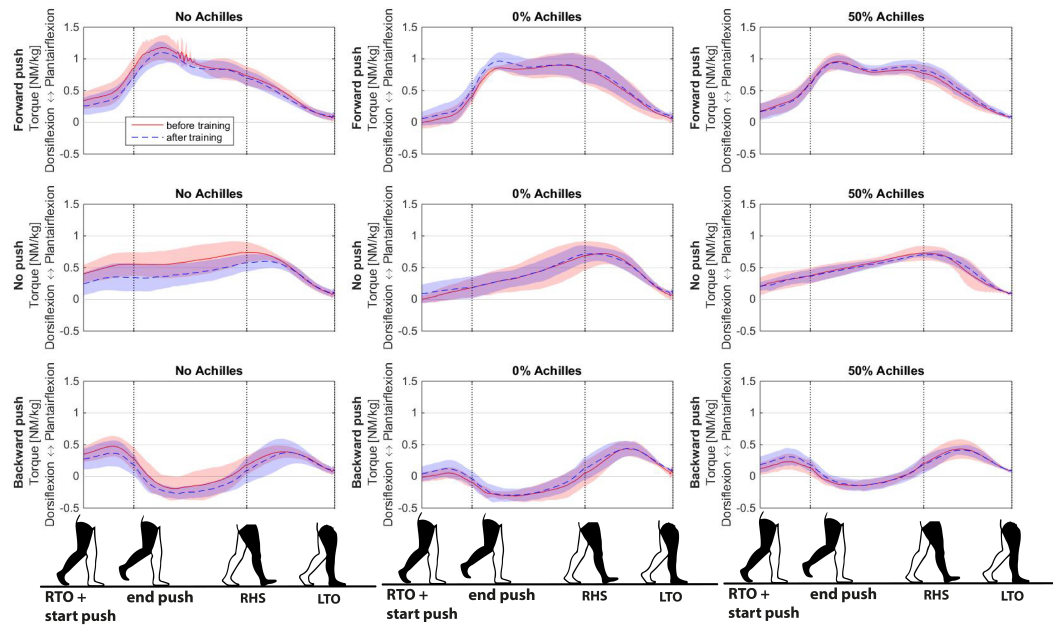


Figure 36: Comparing the total torque values around the ankle (Achilles with muscles+ligaments) of the 8 pushes before and the 8 pushes after the training of 6 subjects. It is normalized in weight and in time for each gait phase indicated at the x-axis.

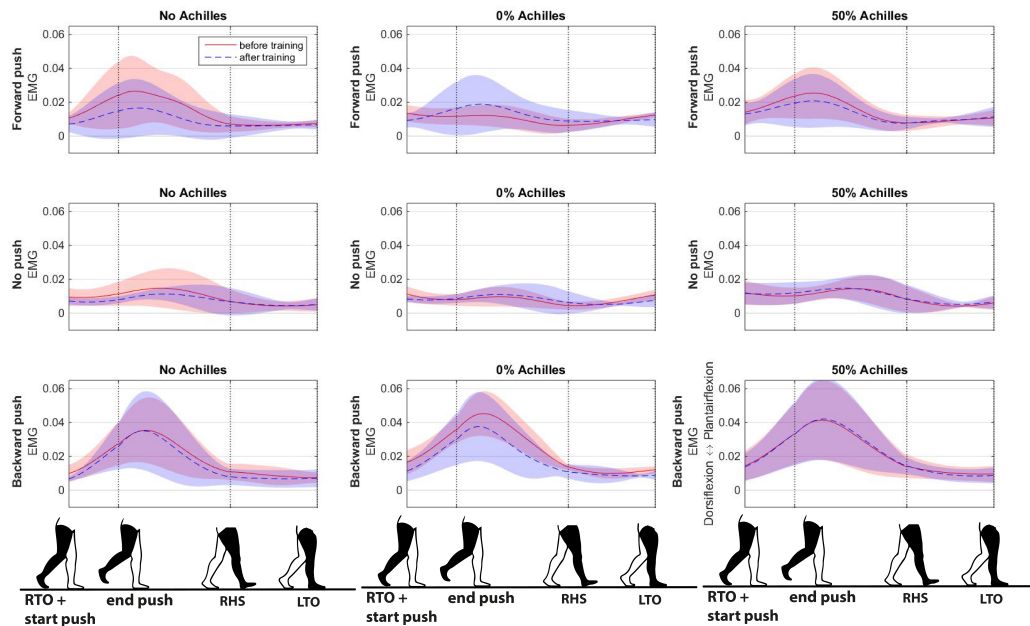


Figure 37: EMG SOL of the 8 pushes before and the 8 pushes after the training of 6 subjects. It was normalized in time for each gait phase indicated at the x-axis.

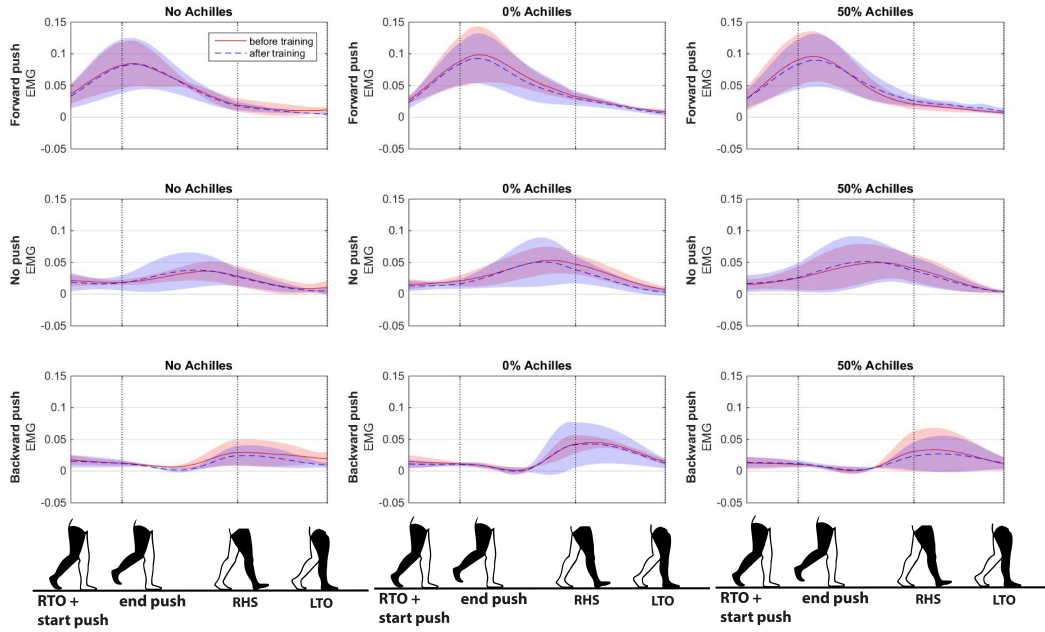


Figure 38: EMG GAS of the 8 pushes before and the 8 pushes after the training of 6 subjects. It was normalized in time for each gait phase indicated at the x-axis.

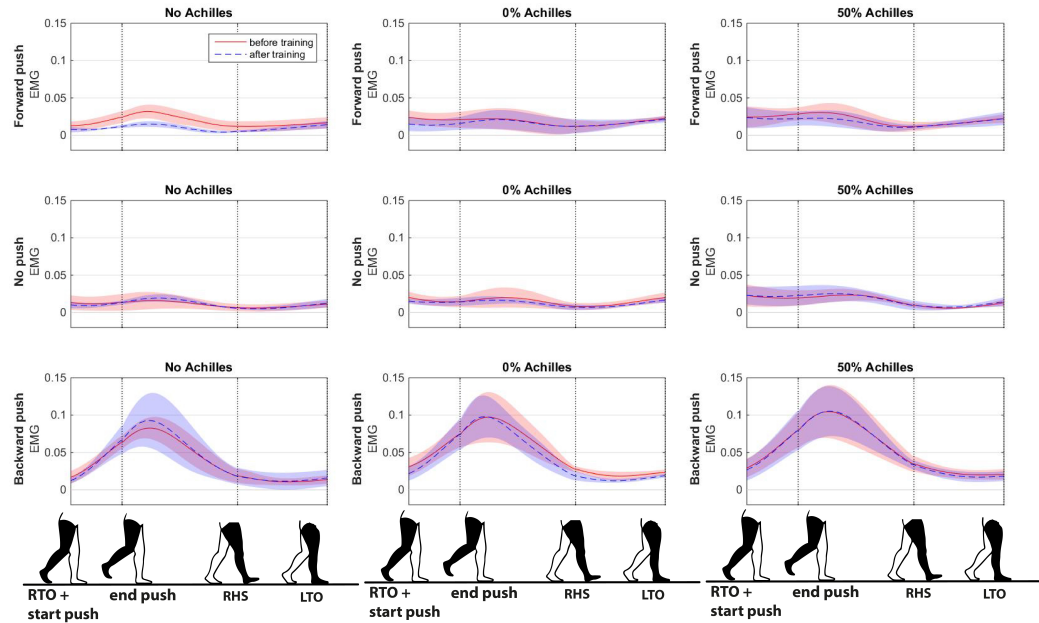


Figure 39: EMG TA of the 8 pushes before and the 8 pushes after the training of 6 subjects. It was normalized in time for each gait phase indicated at the x-axis.

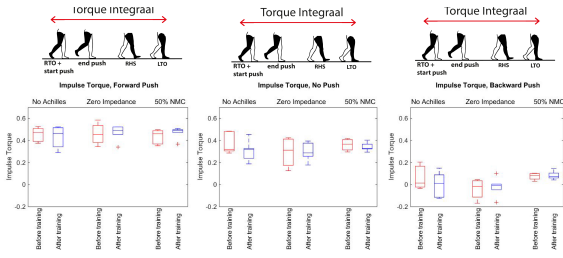


Figure 40: Boxplot of the integral of the total torque (Achilles + muscles and ligaments) of 6 subjects from the 8 pushes before and the 8 pushes after the training. Taken from the Push until LTO.

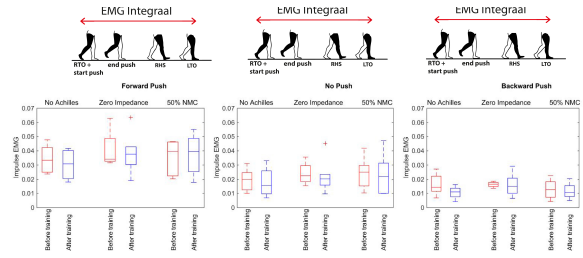


Figure 43: Boxplot of the integral of the EMG of the GAS of 6 subjects from the 8 pushes before and the 8 pushes after the training. Taken from the Push until LTO.

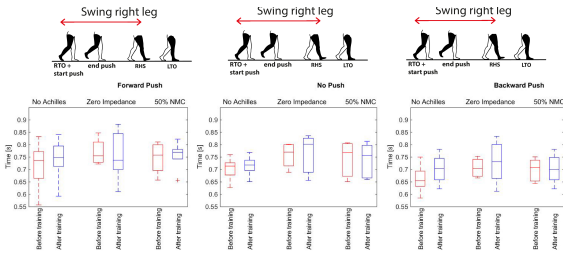


Figure 41: Boxplot of the right swing duration of 6 subjects from the 8 pushes before and the 8 pushes after the training. Taken from the Push until RHS.

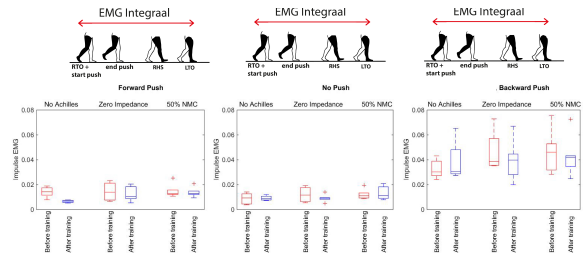


Figure 44: Boxplot of the integral of the EMG of the TA of 6 subjects from the 8 pushes before and the 8 pushes after the training. Taken from the Push until LTO.

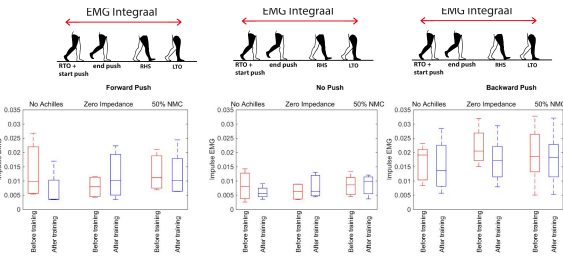


Figure 42: Boxplot of the integral of the EMG of the SOL of 6 subjects from the 8 pushes before and the 8 pushes after the training. Taken from the Push until LTO.

Extra figures of all subjects averaged, only from the 8 pushes after the training.

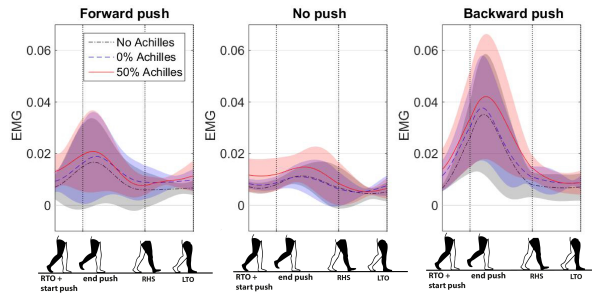


Figure 45: EMG SOL of the 8 pushes after the training. It was normalized in time for each gait phase indicated at the x-axis.

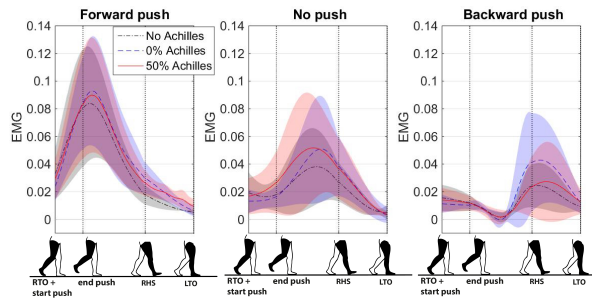


Figure 46: EMG GAS of the 8 pushes after the training. It was normalized in time for each gait phase indicated at the x-axis.

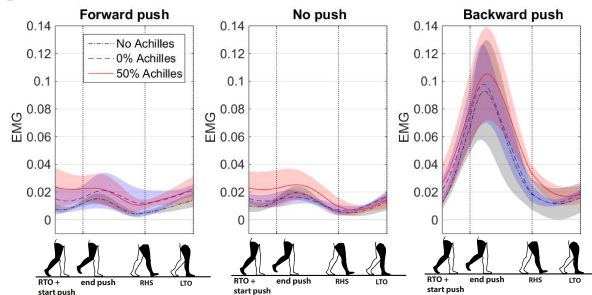


Figure 47: EMG TA of the 8 pushes after the training. It was normalized in time for each gait phase indicated at the x-axis.

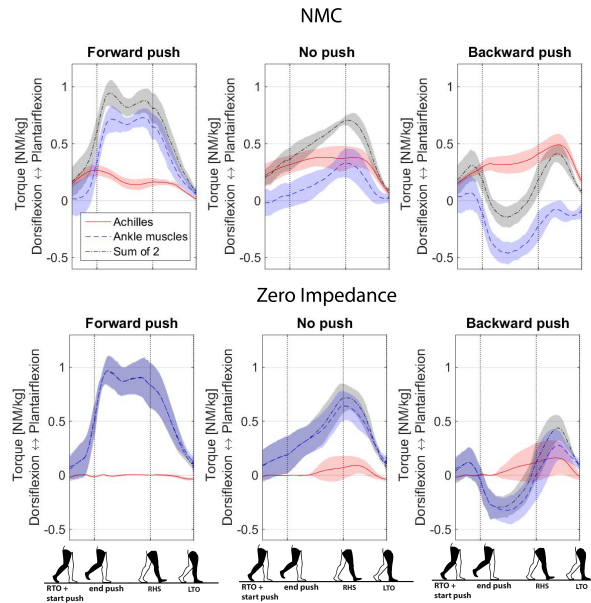


Figure 48: The total torque around the ankle (Achilles + muscles and ligaments), the Achilles torque measured and the torque delivered by the muscles and ligaments (calculated by subtracting the Achilles torque from the total torque). The data is from the 8 pushes after the training. It was normalized in time for each gait phase indicated at the x-axis.

Subject specific graphs, the Torque

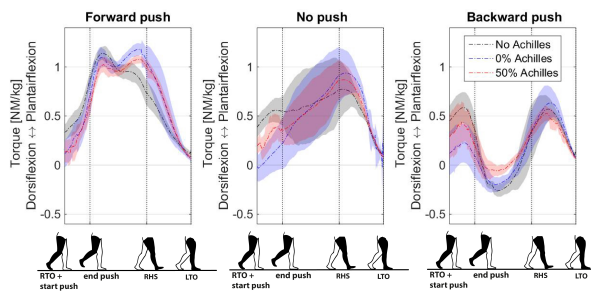


Figure 49: The total torque around the ankle (Achilles + muscles and ligaments). The data is from the 8 pushes after the training from subject 1. It was normalized in time for each gait phase indicated at the x-axis.

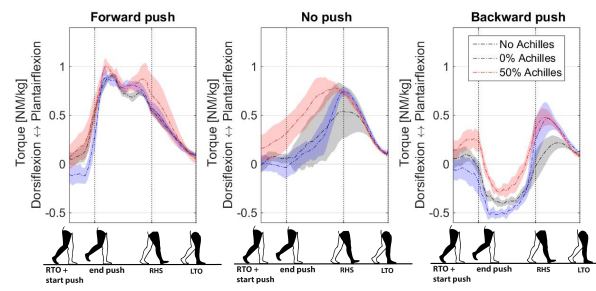


Figure 52: The total torque around the ankle (Achilles + muscles and ligaments). The data is from the 8 pushes after the training from subject 4. It was normalized in time for each gait phase indicated at the x-axis.

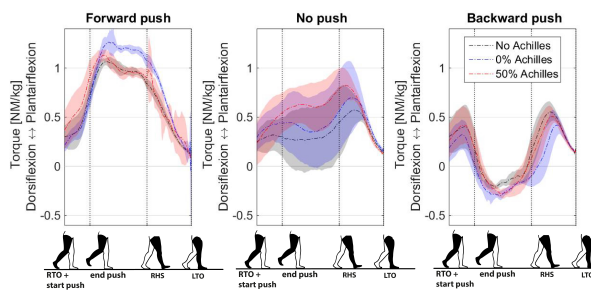


Figure 50: The total torque around the ankle (Achilles + muscles and ligaments). The data is from the 8 pushes after the training from subject 2. It was normalized in time for each gait phase indicated at the x-axis.

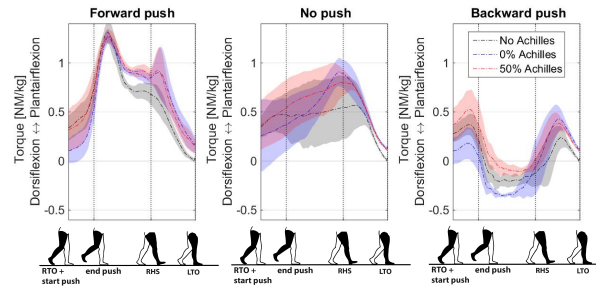


Figure 53: The total torque around the ankle (Achilles + muscles and ligaments). The data is from the 8 pushes after the training from subject 5. It was normalized in time for each gait phase indicated at the x-axis.

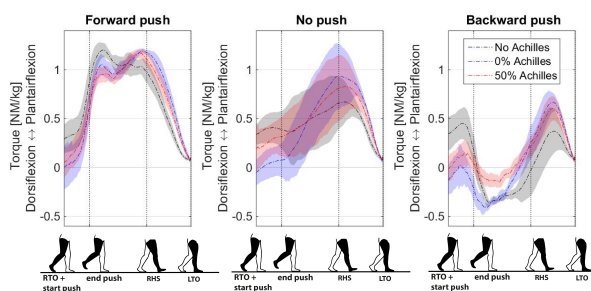


Figure 51: The total torque around the ankle (Achilles + muscles and ligaments). The data is from the 8 pushes after the training from subject 3. It was normalized in time for each gait phase indicated at the x-axis.

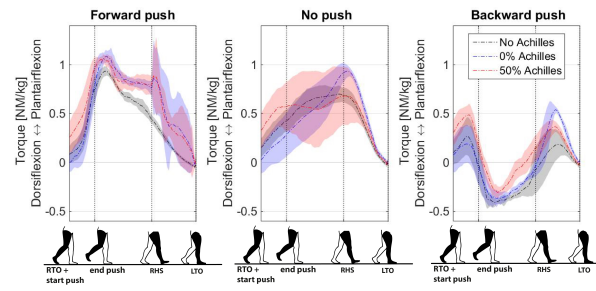


Figure 54: The total torque around the ankle (Achilles + muscles and ligaments). The data is from the 8 pushes after the training from subject 6. It was normalized in time for each gait phase indicated at the x-axis.

Subject specific graphs, the SOL

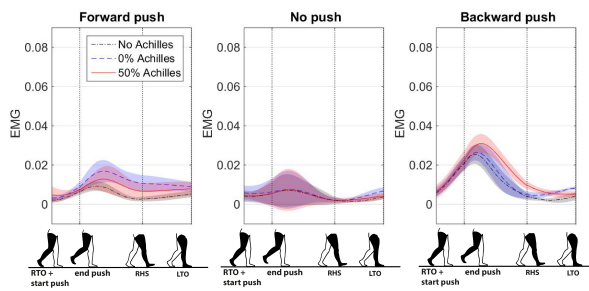


Figure 55: The EMG of the SOL. The data is from the 8 pushes after the training from subject 1. It was normalized in time for each gait phase indicated at the x-axis.

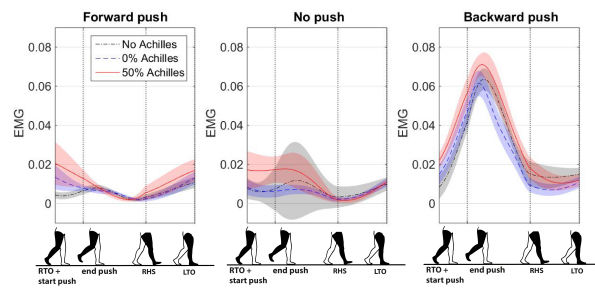


Figure 58: The EMG of the SOL. The data is from the 8 pushes after the training from subject 4. It was normalized in time for each gait phase indicated at the x-axis.

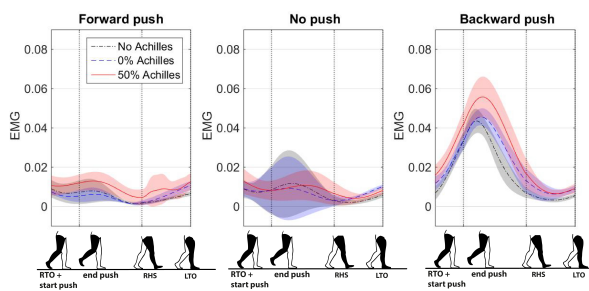


Figure 56: The EMG of the SOL. The data is from the 8 pushes after the training from subject 2. It was normalized in time for each gait phase indicated at the x-axis.

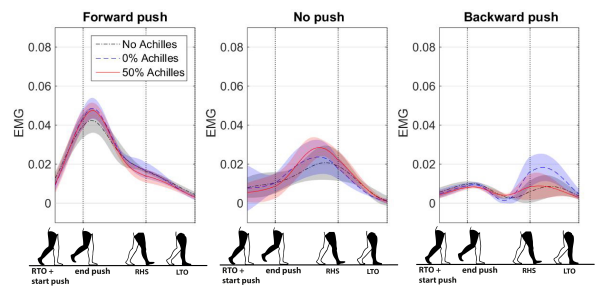


Figure 59: The EMG of the SOL. The data is from the 8 pushes after the training from subject 5. It was normalized in time for each gait phase indicated at the x-axis.

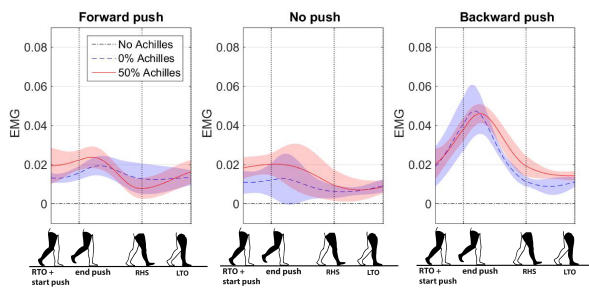


Figure 57: The EMG of the SOL. The data is from the 8 pushes after the training from subject 3. It was normalized in time for each gait phase indicated at the x-axis.

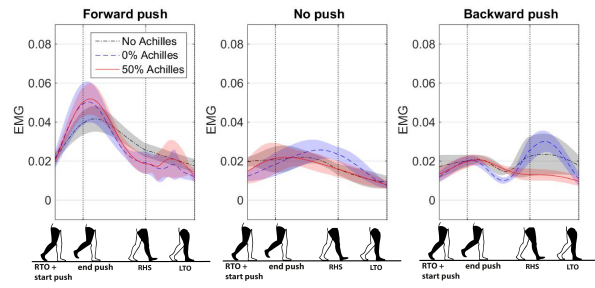


Figure 60: The EMG of the SOL. The data is from the 8 pushes after the training from subject 6. It was normalized in time for each gait phase indicated at the x-axis.

Subject specific graphs, the GAS

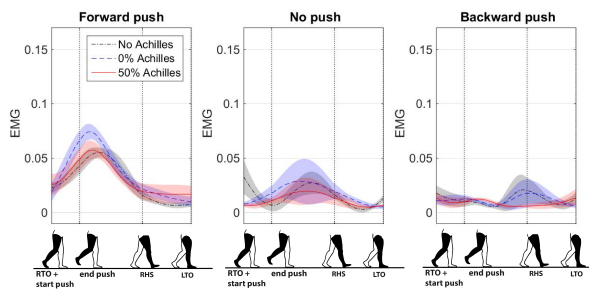


Figure 61: The EMG of the GAS. The data is from the 8 pushes after the training from subject 1. It was normalized in time for each gait phase indicated at the x-axis.

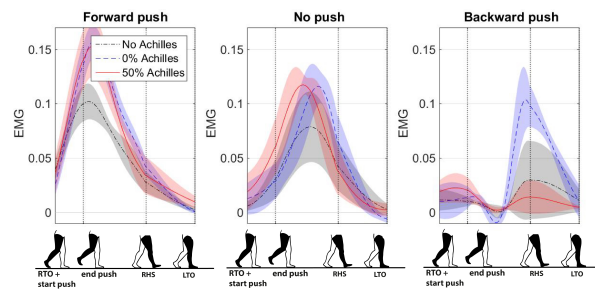


Figure 64: The EMG of the GAS. The data is from the 8 pushes after the training from subject 4. It was normalized in time for each gait phase indicated at the x-axis.

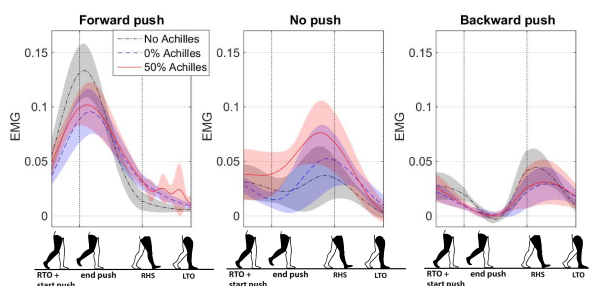


Figure 62: The EMG of the GAS. The data is from the 8 pushes after the training from subject 2. It was normalized in time for each gait phase indicated at the x-axis.

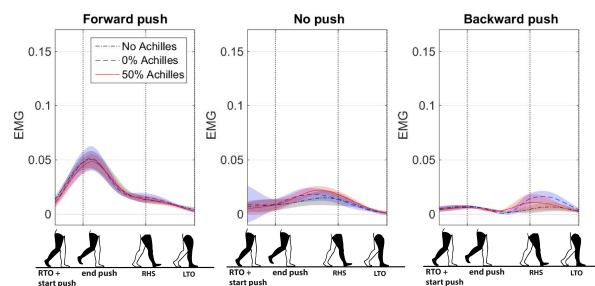


Figure 65: The EMG of the GAS. The data is from the 8 pushes after the training from subject 5. It was normalized in time for each gait phase indicated at the x-axis.

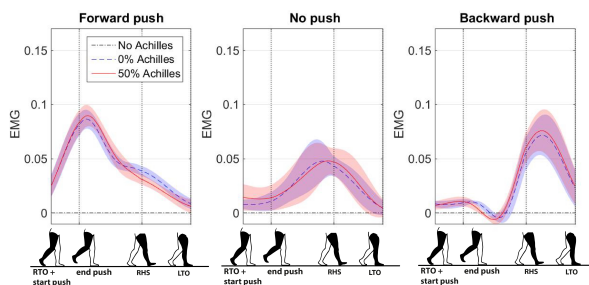


Figure 63: The EMG of the GAS. The data is from the 8 pushes after the training from subject 3. It was normalized in time for each gait phase indicated at the x-axis.

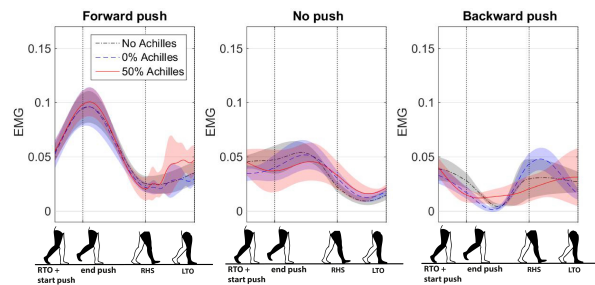


Figure 66: The EMG of the GAS. The data is from the 8 pushes after the training from subject 6. It was normalized in time for each gait phase indicated at the x-axis.

Subject specific graphs, the TA

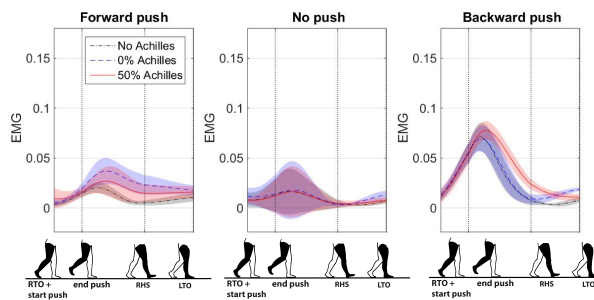


Figure 67: The EMG of the TA. The data is from the 8 pushes after the training from subject 1. It was normalized in time for each gait phase indicated at the x-axis.

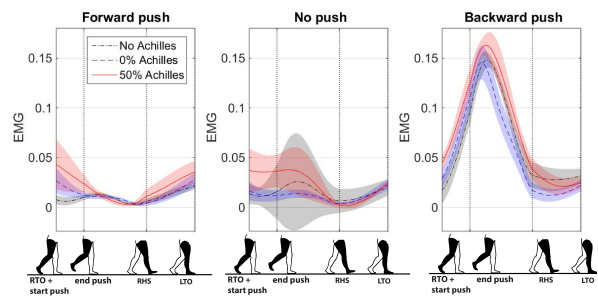


Figure 70: The EMG of the TA. The data is from the 8 pushes after the training from subject 4. It was normalized in time for each gait phase indicated at the x-axis.

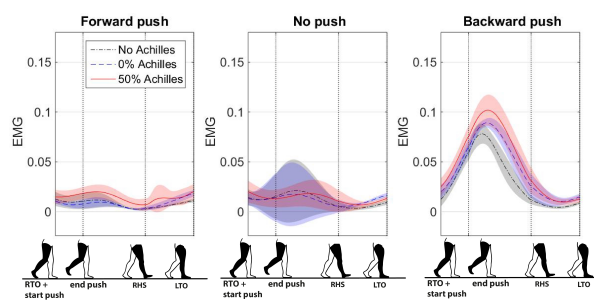


Figure 68: The EMG of the TA. The data is from the 8 pushes after the training from subject 2. It was normalized in time for each gait phase indicated at the x-axis.

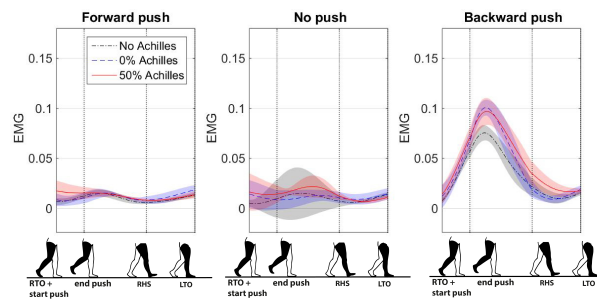


Figure 71: The EMG of the TA. The data is from the 8 pushes after the training from subject 5. It was normalized in time for each gait phase indicated at the x-axis.

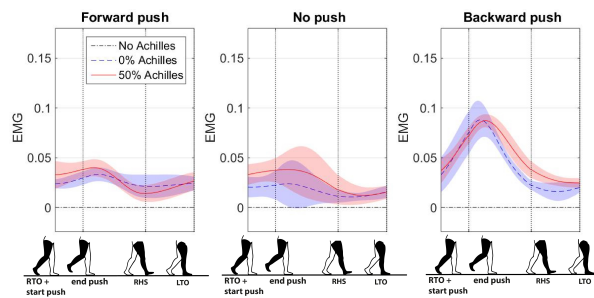


Figure 69: The EMG of the TA. The data is from the 8 pushes after the training from subject 3. It was normalized in time for each gait phase indicated at the x-axis.

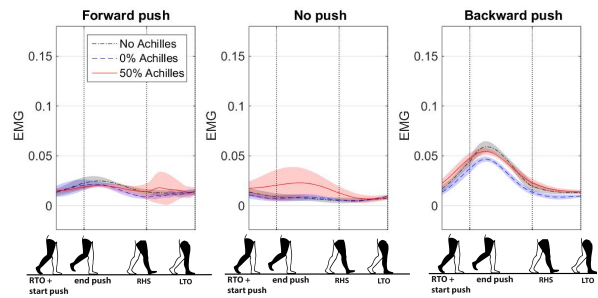


Figure 72: The EMG of the TA. The data is from the 8 pushes after the training from subject 6. It was normalized in time for each gait phase indicated at the x-axis.